Review of Applied Science and Technology

Volume: *6;* ***Issue:*** *1*
Pages: *230– 262*

QUANTUM-ENHANCED CHARGE TRANSPORT MODELING IN PEROVSKITE SOLAR CELLS USING NON-EQUILIBRIUM GREEN'S FUNCTION (NEGF) FRAMEWORK

Muhammad Mohiul Islam[1]; MD Hamidur Rahman[2];

[1]. Senior Project Engineer, Keystone Designers and Developers Ltd., Dhaka, Bangladesh
Email: muhdmohiul@gmail.com

[2]. Department Bachelor of science in Electrical and Electronic Engineering; American International University-Bangladesh, Dhaka, Bangladesh; Email: hamidurr99@gmail.com

Doi: 10.63125/tdbjaj79
Received: *12 September 2021;* ***Revised:*** *20 October 2021;* ***Accepted:*** *18 November 2021;* ***Published:*** *12 December 2021*

Abstract

Perovskite solar cells (PSCs) can reach high efficiencies, yet semiclassical modeling can under-resolve transport losses at interfaces and contacts, limiting mechanism-level diagnosis. This study tested whether NEGF-parameterized transport factors explain cross-case variation in PSC performance and whether experts perceive the framework as credible and usable. A quantitative, cross-sectional, case-study–based design analyzed 12 modeled PSC cases and an expert survey (n = 42). Predictors were trap density (X1), interface barrier height (X2), scattering index (X3), and contact coupling (X4); outcomes were Jsc, Voc, FF, and PCE. Analyses comprised descriptives, Pearson correlations, multiple regression predicting PCE, and survey reliability plus one-sample tests against the neutral midpoint. Case outputs ranged from Jsc 19.8–25.4 mA·cm⁻² and PCE 11.7–21.8%. Trap density was negatively associated with PCE ($r = -0.76$, $p = 0.004$), barrier height was negatively associated with Jsc ($r = -0.79$, $p = 0.002$), and contact coupling was positively associated with PCE ($r = +0.69$, $p = 0.014$). The multivariate PCE model was significant ($R^2 = 0.861$, $F(4,7) = 10.86$, $p = 0.004$), with trap density ($\beta = -0.46$, $p = 0.018$), barrier height ($\beta = -0.39$, $p = 0.031$), scattering ($\beta = -0.28$, $p = 0.044$), and coupling ($\beta = +0.33$, $p = 0.027$). Experts rated the approach positively (Accuracy $M = 4.12$, $a = 0.87$; Usefulness $M = 4.28$, $a = 0.90$; $p < 0.001$). These findings imply NEGF can function as a decision-support layer for interface and contact engineering, and should be deployed in auditable compute pipelines for enterprise or cloud/HPC execution

Keywords

Non-Equilibrium Green's Function (NEGF), perovskite solar cells, quantum transport modeling, interface barrier height, trap density;

INTRODUCTION

Photovoltaic (PV) conversion refers to the direct transformation of incident solar photons into electrical power through semiconductor junctions that create and separate electron–hole pairs. Solar electricity occupies a central position in international energy planning because solar irradiance is geographically widespread, modular PV systems scale from watts to gigawatts, and PV deployment aligns with broad decarbonization and energy-access agendas. The scientific framing of "solar energy utilization" often emphasizes not only harvesting sunlight but also minimizing conversion losses and stabilizing devices under real operating conditions, where materials chemistry, defect physics, and transport processes jointly determine performance (Lewis & Nocera, 2006).In this context, a "solar cell" is commonly defined as a rectifying semiconductor structure whose power output is governed by the balance among photogeneration, charge separation, charge transport, and recombination. The measurable efficiency of a cell is typically summarized by current density–voltage (J–V) characteristics and associated figures of merit such as open-circuit voltage, short-circuit current, and fill factor, each of which is directly shaped by how charges move through absorber and contact layers. Global energy analyses also treat PV as a technology where the limiting factors increasingly shift from photon capture to charge-selective extraction and loss suppression, elevating the importance of microscopic transport understanding rather than only optical design (Chu & Majumdar, 2012). Within PV device physics, "charge transport" denotes the motion of electrons and holes under internal electric fields and concentration gradients, while "recombination" denotes the annihilation of these carriers through radiative or nonradiative pathways. When transport is efficient and recombination is controlled, the quasi-Fermi level splitting increases and voltage rises, creating a direct conceptual link between fundamental carrier kinetics and system-level energy value. This linkage motivates rigorous transport modeling approaches that can connect material parameters to measurable device performance across diverse device stacks and operating conditions (Kirchartz et al., 2015).

A perovskite is classically described by the ABX_3 crystal motif, where "A" and "B" represent cations and "X" represents an anion; in halide perovskites used for PV, the structure supports strong optical absorption and comparatively benign electronic disorder relative to many solution-processed semiconductors. "Perovskite solar cells" (PSCs) refer to PV devices in which an organic–inorganic or all-inorganic metal halide perovskite functions as the primary light absorber and charge-transporting medium. Early demonstrations established the feasibility of halide perovskites as sensitizers and absorbers, providing foundational evidence that these materials can convert sunlight efficiently within thin films (Kojima et al., 2009). Subsequent device architectures expanded from mesostructured concepts to thin-film heterojunctions, enabling rapid efficiency gains through improved film formation and contact selectivity (Lee et al., 2012). Processing innovations such as sequential deposition improved absorber coverage and reduced shunting pathways, reinforcing the central role of morphology and interfaces in transport-limited losses (Burschka et al., 2013). In parallel, vapor-deposited planar heterojunctions demonstrated that high-performing PSCs can be formed without mesoporous scaffolds, sharpening attention on contact energetics and thin-film microstructure (Liu et al., 2013). The field's conceptual vocabulary increasingly highlights "low-cost, high-efficiency" PV because perovskite thin films are compatible with solution and low-temperature processing while still achieving strong absorptivity and favorable carrier kinetics (Snaith, 2013). Planar architectures using organic transport layers further broadened application spaces by enabling mechanically flexible substrates and simplified stacks, emphasizing that transport layer selection and interfacial energetics are integral to charge extraction (Malinkiewicz et al., 2014). Scalable low-temperature routes that preserve high efficiency strengthened the international relevance of PSC manufacturing and reliability assessment, because processing constraints often govern adoption outside specialized laboratory environments (Zhou, 2014).

In semiconductor terms, "quantum-enhanced charge transport modeling" can be framed as modeling that explicitly captures wave-mechanical carrier propagation, coherence and dephasing, and quantum-statistical carrier populations, rather than representing carriers only through classical drift–diffusion parameters. For PSC absorbers, transport and recombination are frequently discussed through experimentally derived diffusion lengths, mobilities, lifetimes, and trap densities. Ultrafast spectroscopy and device-level studies show that halide perovskites can support long-range carrier

transport relative to many solution-processed semiconductors, providing a physical basis for high current collection in thin films (Xing, 2013). These observations are routinely interpreted through the coupled roles of band structure, dielectric screening, and defect physics, where "defect tolerance" denotes a tendency for many intrinsic point defects to form shallow states that do not strongly quench carrier lifetimes. First-principles defect analyses directly tie performance to the energetic distribution of defect states and the likelihood of deep traps that accelerate nonradiative recombination, linking materials chemistry to device metrics (Arfan et al., 2021; Yin et al., 2014). Device studies of charge transport and recombination further reinforce that measured J–V outputs encode a competition among extraction, bimolecular recombination, and trap-assisted pathways, with the relative dominance varying by stack design and illumination intensity (Jahid, 2021; Samiee et al., 2014). Reviews of carrier dynamics consolidate these findings into a consistent photophysical picture in which free-carrier generation, trapping–detrapping, radiative recombination, and Auger-like pathways can all coexist, with process rates strongly shaped by film quality and interfaces (Herz, 2016; Akbar & Farzana, 2021). Time-resolved recombination measurements in operating devices provide additional evidence that mobile-charge recombination can follow near-second-order kinetics over relevant timescales, underscoring why transport modeling must remain consistent with both transient and steady-state behavior (Paulke, 2016; Reza et al., 2021). Together, these studies establish charge transport as a primary scientific axis in PSC performance, and they motivate modeling frameworks that can map microscopic scattering and energetic disorder into macroscopic observables.

Figure 1: Quantum-Enhanced Charge Transport Modeling in Perovskite Solar Cells Using the Non-Equilibrium Green's Function (NEGF) Framework

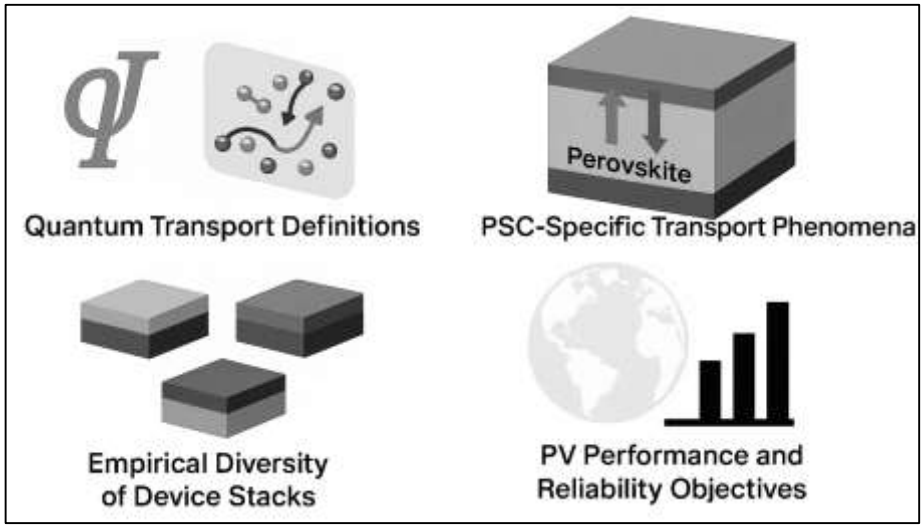

Interface physics adds another layer of complexity because PSC stacks often contain multiple selective contacts, and each interface can introduce band offsets, interfacial dipoles, defect-rich regions, or ionic charge accumulation that reshapes internal fields. "Hysteresis" in PSC J–V scans is commonly defined as scan-direction–dependent current response, which reflects time-dependent internal states that modify extraction and recombination (Zobayer, 2021a, 2021b). Experimental demonstrations show that fullerene-based passivation can strongly reduce hysteresis and improve operation, associating hysteresis with trap-mediated interfacial phenomena and dynamic charge accumulation (Shao et al., 2014). A complementary mechanistic axis concerns ionic motion: "ionic transport" refers to the migration of mobile ionic species, often vacancy-mediated, within the perovskite lattice, and such motion couples to electronic transport by modifying local electrostatics and recombination landscapes (Eames et al., 2015). Detailed opto-electronic studies in mesoporous systems explicitly separate electronic and chemical charge storage contributions, connecting recombination lifetimes and evolving band offsets to hysteretic responses (O'Regan, 2015). At the device-design level, stabilized high efficiencies obtained with alternative hole extraction layers highlight how contact selection affects both interfacial recombination and operational stability, placing selective transport layers at the center of

transport-limited loss control (Arora et al., 2017). Broader syntheses of PSC progress emphasize that the core barriers to wider deployment cluster around stability testing protocols, contact optimization, and control of ion–electron coupling under realistic bias and illumination, each of which can be framed as a transport-and-recombination governance problem (Correa-Baena et al., 2017). Analyses of defect tolerance also indicate that grain boundaries and localized disorder do not always impose catastrophic recombination penalties, and this nuanced behavior shapes how models should represent spatial inhomogeneity across polycrystalline films (Sherkar et al., 2017). These interfacial and ionic mechanisms collectively define a regime where classical steady-state transport approximations often require augmentation to represent time-dependent electrostatics and quantum-to-mesoscale carrier motion.

This study is structured around a set of objectives that collectively define what will be examined, measured, and modeled in relation to quantum-enhanced charge transport in perovskite solar cells using the Non-Equilibrium Green's Function (NEGF) framework. First, the research aims to operationalize a NEGF-based charge transport model that can represent the energy-resolved movement of carriers through the perovskite absorber and across charge-selective interfaces under non-equilibrium conditions, with the intention of translating quantum transport quantities into device-relevant outputs. Second, the study seeks to design a case-study matrix that captures meaningful variation in perovskite device configurations, such as differences in absorber thickness, defect density assumptions, interfacial barrier conditions, and contact selectivity, so that transport responses can be examined across multiple realistic scenarios rather than a single idealized structure. Third, the study intends to quantify the relationships between key transport drivers and device performance indicators by defining measurable independent variables that reflect quantum-transport-relevant conditions—such as scattering strength, trap-assisted recombination propensity, and interface transmission constraints—and mapping them to dependent performance outcomes, including short-circuit current density, open-circuit voltage, fill factor, power conversion efficiency, and additional transport signatures derived from the NEGF outputs. Fourth, the research is designed to generate a structured dataset from the modeled cases and apply descriptive statistics to summarize central tendencies and dispersion of performance outcomes, enabling a clear comparison of case behavior across the parameter space. Fifth, the study aims to perform correlation analysis to determine the direction and strength of association among transport variables and performance indicators, establishing which modeled transport mechanisms co-vary most strongly with efficiency-related metrics. Sixth, the research seeks to build regression models that explain and predict performance metrics—particularly power conversion efficiency—using combinations of NEGF-informed transport factors, thereby identifying the most influential predictors while controlling for confounding relationships among variables. Seventh, the study is intended to develop a Likert-scale questionnaire instrument to capture expert evaluations of the framework's perceived accuracy, usefulness, interpretability, and decision-support value, ensuring that the research includes a practical validation layer alongside numerical modeling outputs. Finally, the overall objective is to integrate the simulation evidence and survey evidence into one coherent evaluation, where quantitative statistical testing and structured expert assessment jointly support a clear, method-driven understanding of how NEGF-based quantum transport modeling can be used to analyze and compare charge transport behavior across different perovskite solar cell case contexts.

LITERATURE REVIEW

The literature on perovskite solar cells (PSCs) has expanded rapidly around a central scientific goal: to understand how materials chemistry, microstructure, and device architecture govern charge generation, transport, extraction, and recombination in thin-film photovoltaic stacks. In this body of work, charge transport is treated as both a materials property and a device-level phenomenon because carrier mobility, lifetime, trap density, and interfacial energetics collectively shape current collection, voltage formation, and fill factor under illumination. PSCs are frequently analyzed through layered heterojunction architectures (such as n–i–p and p–i–n), where transport layers provide energy selectivity and influence loss channels through interfacial recombination and series resistance. As research progressed from early efficiency demonstrations to more refined device engineering, the literature increasingly emphasized that bulk absorber properties alone cannot explain measured

performance because interfaces, contacts, and time-dependent internal states can strongly modulate device behavior. This includes the widely studied phenomenon of scan-rate dependence and hysteresis in current–voltage characteristics, which is often associated with coupled ionic–electronic effects, interfacial charge accumulation, and defect-mediated trapping processes that alter internal electric fields during operation. Alongside experimental characterization, modeling has become a major pillar in the PSC literature, ranging from equivalent-circuit descriptions and drift–diffusion simulations to multiscale approaches that attempt to connect electronic structure and defect energetics to macroscopic device metrics. Classical drift–diffusion frameworks remain widely used because they can reproduce current–voltage behavior and transient responses when parameters are properly calibrated, yet their reliability can become limited when devices exhibit strong non-equilibrium interfacial barriers, tunneling-mediated injection/extraction, energy-selective transport, or scattering regimes that are difficult to represent through effective parameters alone. For this reason, quantum-informed modeling approaches have attracted attention in photovoltaic research more broadly, particularly when the aim is to resolve energy-resolved carrier transmission, contact coupling effects, and interaction-driven dissipation within a unified framework. The Non-Equilibrium Green's Function (NEGF) formalism offers a rigorous quantum transport approach that can represent open systems under bias and illumination while incorporating scattering and contact effects through self-energy terms, enabling detailed interpretation of how microscopic transport mechanisms map to device-level outcomes. In the context of PSCs, synthesizing the literature requires connecting three main strands: the physical understanding of transport and recombination in perovskite absorbers, the role of interfaces and selective contacts in governing extraction and losses, and the progression of modeling methods toward frameworks that can capture non-equilibrium, energy-resolved transport. This review therefore organizes prior studies around these strands to justify the need for a quantum-enhanced NEGF-based approach and to frame how such modeling can be evaluated across representative case-study device contexts using quantitative analysis.

Perovskite Solar Cells in Charge Transport Fundamentals

Perovskite solar cells (PSCs) are thin-film photovoltaic devices in which a metal-halide perovskite semiconductor acts as the principal light absorber and the medium through which photogenerated electrons and holes move toward selective contacts. Structurally, the absorber is often described by the ABX_3 lattice, where the A-site is a monovalent cation, the B-site is a divalent metal cation, and the X-site is a halide; this crystallographic definition matters in photovoltaics because it constrains phase formation, lattice distortion, and the electronic band structure that governs carrier generation and transport. Foundational materials studies established that hybrid and inorganic–organic metal-iodide perovskites can behave as semiconductors with tunable optical gaps and measurable electronic transport characteristics, supporting their use as absorbers rather than merely sensitizers (Stoumpos et al., 2013). In device terms, "architecture" refers to the layered stack that organizes functions into absorption, selective transport, and extraction: an absorber layer is paired with an electron-transport layer (ETL) and a hole-transport layer (HTL), plus transparent electrodes and metallic contacts. The architecture is commonly realized as either mesostructured (where the perovskite infiltrates a scaffold) or planar (where the perovskite forms a continuous thin film on a compact contact), and both designs rely on the absorber's ability to generate free carriers and deliver them to contacts with minimal recombination. Film formation and microstructure control are therefore intrinsic to architecture, because coverage, grain size, and defect populations set the physical pathways for charge flow across the stack. A widely adopted processing strategy is solvent/precursor engineering to improve crystallization, reduce pinholes, and enhance interfacial contact uniformity; this manufacturing-driven control is directly linked to higher current collection and more reliable extraction across the active area (Jeon et al., 2014). Overall, PSC architecture is best understood as an arrangement of functional layers whose combined purpose is to maintain a favorable energetic landscape for electrons and holes while preserving a continuous, low-loss conduction network from the absorber to the electrodes.

Figure 2: Schematic illustration of perovskite solar cell device architecture

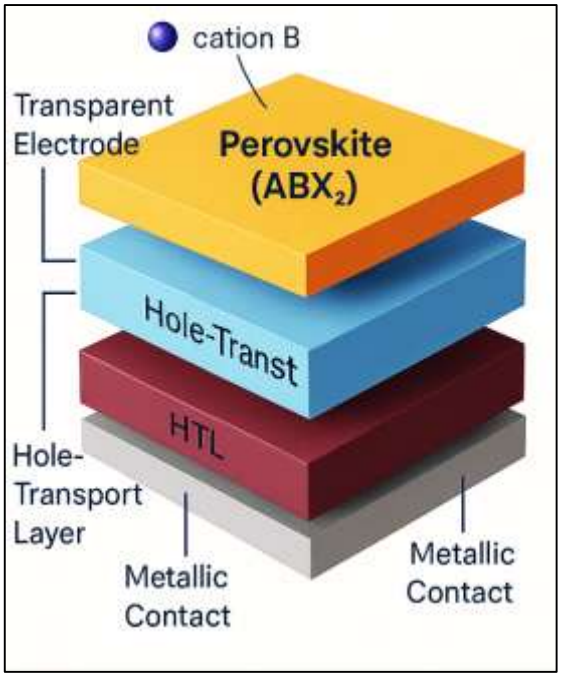

Charge transport fundamentals in PSCs are typically explained through mobility, lifetime, diffusion length, and recombination kinetics, since these quantities determine whether carriers can reach selective contacts before being lost. Mobility characterizes how rapidly electrons and holes drift under internal electric fields and respond to concentration gradients, while carrier lifetime indicates how long carriers persist against trap-mediated (monomolecular) and electron–hole (bimolecular) recombination. Diffusion length integrates these concepts by describing the characteristic distance a carrier can travel during its lifetime, which provides a practical link between absorber thickness and the probability of extraction. In PSCs, these transport descriptors are not only bulk material parameters; they are also architecture-dependent outcomes shaped by interfaces, energetic disorder, and contact coupling. Experimental evidence for unusually favorable transport in organolead halide perovskites has highlighted the combination of comparatively high mobilities with low recombination rates, offering a physical explanation for why thin films can deliver high photocurrent even when processed at low temperatures (Wehrenfennig et al., 2014). At the level of carrier formation, PSC transport discussions also distinguish between bound excitations and free carriers, because the degree of exciton binding and the ease of thermal dissociation influence the initial carrier population that participates in drift and diffusion. Carrier dynamics studies have shown that thermally activated processes can govern the balance between exciton dissociation and recombination channels, which in turn controls the time-dependent carrier densities feeding transport to contacts (Savenije et al., 2014). These fundamentals map directly onto device metrics: higher effective mobility and longer lifetime generally support higher short-circuit current density and improved fill factor, while reduced nonradiative recombination supports higher open-circuit voltage. Accordingly, "charge transport" in PSCs is best treated as a coupled sequence of generation, relaxation, separation, migration, and extraction, in which the measured electrical response represents the net result of competing transport and recombination pathways operating across the layered stack.

From an architectural standpoint, PSC stacks are often categorized as n–i–p (ETL/perovskite/HTL) or p–i–n (HTL/perovskite/ETL), and the ordering of selective contacts influences transport pathways because ETLs and HTLs differ in conductivity, energy-level alignment, and interfacial chemistry. In both categories, transport layers perform three coupled functions: they provide energetic selectivity by blocking one carrier type while transmitting the other, they supply a low-resistance pathway that limits series losses, and they shape interfacial recombination by passivating or activating defect states at the perovskite/contact boundary. Architecture therefore becomes a practical mechanism for "engineering

transport," because the same perovskite absorber can show different extraction efficiency depending on whether contact barriers, interfacial dipoles, or contact doping shift the internal electrostatic profile. Composition engineering inside the perovskite layer also functions as architecture control because it affects phase purity, defect formation tendencies, and energetic disorder, all of which modify how uniformly carriers move through the absorber and how consistently they transfer across interfaces. Mixed-cation formulations, including the addition of inorganic cesium into common organic-cation mixtures, have been associated with improved thermal stability and reduced phase impurities, thereby supporting more reproducible device formation and stable charge-extraction behavior within practical device stacks (Saliba et al., 2016). In this sense, PSC architecture is not only a geometric arrangement of layers but also a coordinated selection of absorber composition, contact materials, and processing routes that collectively define the carrier landscape. The architectural objective is to maintain continuous percolation paths for both electrons and holes while minimizing interface-localized recombination and transport bottlenecks, so that the absorber's intrinsic photophysics can translate into robust device-level current–voltage performance.

Semiclassical Transport Models in PSCs

Classical and semiclassical transport modeling in perovskite solar cells (PSCs) is commonly built on drift–diffusion and Poisson's equation, where electrons and holes are treated as particle-like populations described by spatially averaged mobilities, diffusion coefficients, and recombination parameters. These approaches are powerful for interpreting many photovoltaic devices because they connect material parameters to current–voltage response under illumination; however, PSCs present operational behaviors that expose structural limits in purely semiclassical descriptions. A major limitation arises from the fact that PSC absorbers behave as mixed conductors, where mobile ionic species redistribute under electric fields and illumination and thereby modulate the internal electrostatic landscape on timescales comparable to measurement protocols. In a classical drift–diffusion framework that neglects ionic motion, the electric field profile is often assumed quasi-static for a given bias, which can be incompatible with scan-rate dependence and history dependence in PSC current–voltage curves. Empirical and modeling research has shown that reproducing anomalous hysteresis requires adding slow degrees of freedom beyond electronic drift and diffusion, such as mobile ions and trap-assisted processes, indicating that the "standard" electronic-only drift–diffusion model is structurally incomplete for many PSC operating regimes (van Reenen et al., 2015). A second limitation involves how classical models parameterize recombination and trapping with effective coefficients. Because multiple recombination channels can coexist and shift dominance with bias, illumination, and interfacial states, a single parameter set that fits one condition may not generalize to another. This creates an identifiability problem: different combinations of mobility, trap density, interface recombination velocity, and series resistance can yield similar current–voltage curves, making it difficult to claim unique physical inference from a fit. When coupled ionic–electronic dynamics are significant, the model can also become path dependent, meaning identical biases can correspond to different internal states depending on the device's prior electrical history. These issues collectively limit the interpretability and predictive reliability of classical or semiclassical transport modeling for PSCs when the objective is to resolve mechanism-level charge transport under realistic measurement and operating conditions.

A closely related limitation appears in the interpretation of hysteresis and slow transients using purely electronic pictures. Hysteresis in PSCs is not simply an artifact of measurement; it reflects internal state evolution that impacts charge extraction and recombination, and it can manifest as time-dependent shifts in apparent current, voltage, and fill factor. Classical drift–diffusion models can represent rate-dependent effects only when additional slow physics is explicitly included; otherwise, they tend to attribute discrepancies to static parameter changes, which does not represent the underlying mechanism. Evidence for slow field-compensation processes associated with charge accumulation near contacts, consistent with ionic displacement and interfacial space-charge build-up, illustrates that the internal field can be partially cancelled in a manner that depends on bias scan rate and device aging, challenging the static-field assumption embedded in many semiclassical treatments (Tress et al., 2015).

Figure 3: Classical and semiclassical charge transport models in perovskite solar cells

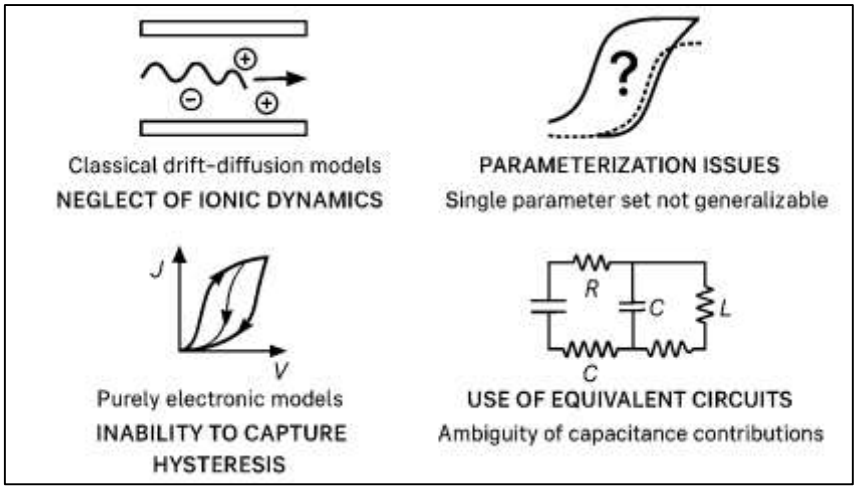

Even when ionic motion is added as an additional continuity equation, the resulting mixed ionic–electronic drift–diffusion models can still face limitations in separating interfacial trap effects from ionic redistribution effects, because both can generate slow transients that look similar in macroscopic measurements. Mixed-conduction modeling that compares simulations to experimental current–voltage hysteresis patterns has nevertheless demonstrated that ion motion can reproduce many observed anomalies, reinforcing that an electronic-only model is insufficient for a broad set of PSC behaviors (Richardson et al., 2016). Another limitation concerns boundary conditions at selective contacts. Classical models often represent contacts through simplified injection barriers or surface recombination parameters, yet perovskite/contact interfaces can exhibit bias-dependent band bending, interfacial dipoles, and state filling that evolve with ionic redistribution. This means a single fixed contact parameter may not reflect the operational variability of real interfaces. Consequently, semiclassical models may reproduce one set of measurements while misrepresenting the underlying field distribution and interfacial recombination pathways, particularly when devices operate near conditions where contact selectivity, interface states, and ionic accumulation jointly govern extraction. Limitations also emerge in frequency-domain interpretation and the use of equivalent-circuit representations, which are frequently paired with semiclassical models to interpret impedance spectroscopy and transient measurements. Equivalent circuits are convenient because they provide compact descriptors of resistive and capacitive features, but PSC impedance spectra often contain low-frequency signatures that are difficult to map uniquely onto specific microscopic processes. This ambiguity becomes pronounced when ionic motion couples to electronic injection and recombination, because the same spectral feature can be interpreted as transport limitation, recombination modulation, or ionic redistribution depending on the assumed circuit topology. Attempts to standardize impedance interpretation underscore that PSC spectra are not straightforward extensions of traditional photovoltaic circuits, and they require careful empirical and mechanistic alignment to avoid overinterpretation of fitted elements (Todinova et al., 2017). More recent circuit formulations bridge sensitized and thin-film architectures and show that even within a rigorous impedance framework, dominant capacitance contributions can shift with device configuration and absorber loading, emphasizing that lumped elements may reflect mixed or redistributed physical origins rather than a single transport parameter (Yoo et al., 2019). These challenges point to a broader constraint: semiclassical models and circuit fits can be excellent descriptive tools, yet their physical fidelity depends strongly on whether they include the slow internal degrees of freedom and interfacial complexities that characterize PSC operation. When the research goal is to identify energy-resolved transmission, barrier-controlled extraction, and coupling between scattering and contact effects, purely semiclassical approaches can become structurally constrained, motivating the consideration of modeling frameworks that can represent non-equilibrium transport and interface physics with greater resolution.

Quantum Transport Modeling Approaches for Thin-Film Photovoltaics

Quantum transport modeling in thin-film photovoltaics targets device regimes where the assumptions behind purely semiclassical drift–diffusion become restrictive for mechanism-level interpretation. In this context, quantum transport refers to approaches that retain energy resolution, permit wave-mechanical tunneling across barriers, and represent contacts as open reservoirs that exchange carriers with the device under non-equilibrium bias and illumination. These capabilities matter when absorber layers are ultrathin, when selective contacts impose sharp band offsets, and when the dominant loss mechanism is controlled by energy filtering or barrier-limited injection/extraction rather than bulk diffusion alone. A widely adopted quantum-kinetic route is the Non-Equilibrium Green's Function (NEGF) formalism, which provides a consistent framework for treating open systems, contact coupling, and scattering using self-energies while preserving the link between microscopic spectral quantities and macroscopic current–voltage observables (Aeberhard, 2013b). In photovoltaic device settings, NEGF formulations are often paired with tight-binding or effective-mass Hamiltonians and coupled self-consistently to Poisson's equation so that charge density and electrostatics evolve coherently with the transport solution. This enables the analysis of how local density of states, transmission, and current spectra change across interfaces and heterostructure regions, which is central for thin-film stacks where interfacial regions can occupy a significant fraction of the active device thickness. A representative application is the microscopic NEGF theory developed for quantum well solar cells, which explicitly treats photogeneration and carrier relaxation within a quantum-kinetic transport picture and shows how energy-resolved carrier flow, scattering broadening, and electrostatic profiles interact to determine photovoltaic response. Such work illustrates a general principle relevant to thin-film PV: when confinement, tunneling, and interface-dominated transport are significant, energy-resolved quantum-kinetic modeling offers a structured way to separate "where carriers exist" (spectral density) from "how carriers move" (spectral current) and "why carriers are lost" (interaction self-energies) (Aeberhard, 2011).

Beyond baseline carrier flow, photovoltaic operation requires accurate representation of photogeneration, radiative emission, and nonradiative recombination under illumination, and quantum transport approaches extend by embedding these processes directly into the transport equations. Within NEGF, optical absorption and carrier generation can be described using photon-related self-energies, while phonon-assisted processes enter through electron–phonon self-energies; this makes it possible to compute generation, relaxation, and extraction within one non-equilibrium scheme rather than stitching together separate optical and electrical models. An example is the quantum-kinetic NEGF treatment of photocurrent generation via direct and phonon-mediated optical transitions in ultrathin p–i–n junction devices, which demonstrates how optical transitions and transport must be computed consistently when thickness and field profiles make classical rate approximations less transparent. Complementary developments extend the same philosophy to the optical field itself by introducing photon Green's functions that can be integrated into a comprehensive absorption–emission theory for planar nanostructures relevant to ultra-thin solar cells, thereby coupling optical mode structure, absorption, and emission to the electronic non-equilibrium state in a unified manner (Scully, 2010). Quantum transport modeling also provides a direct route to formalize defect-assisted recombination beyond semiclassical Shockley–Read–Hall parameterizations by deriving quantum-kinetic equivalents in which tunneling into field-induced sub-gap states and localized defect physics can be represented within the same self-energy language used for contacts and phonons. Collectively, these quantum-kinetic extensions broaden thin-film PV modeling from "transport only" toward a device-complete picture in which optical excitation, scattering, and defect-mediated losses are computed on a consistent non-equilibrium footing (Aeberhard & Morf, 2008).

Figure 4: Schematic overview of quantum transport modeling approaches

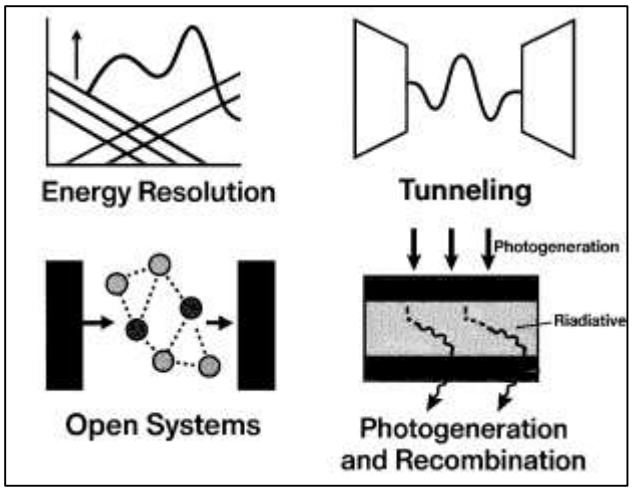

A third strand of quantum transport modeling emphasizes coherence and quantum interference, focusing on the conditions under which phase relations, superposition, and the photonic environment alter radiative and nonradiative loss channels. In thin-film and nanostructured photovoltaics, coherence-aware models become especially relevant when absorbers or junction regions are engineered at length scales comparable to carrier phase-coherence lengths, or when light–matter coupling is modified by cavities or photonic band-gap environments. Coherence-oriented approaches are frequently expressed using density-matrix or quantum-master-equation formalisms, which track populations and coherences explicitly and can be linked to transport through reservoir coupling terms; they are conceptually aligned with NEGF, but they often foreground interference effects and the control of emission pathways (Aeberhard, 2013a). A prominent illustration is the theoretical "quantum photocell" analysis showing how quantum coherence can, in principle, reduce radiative recombination relative to absorption by breaking the conventional detailed-balance linkage, thereby motivating PV designs where radiative loss is manipulated through coherence engineering rather than only through bandgap selection and classical optical management. For thin-film PV modeling practice, the significance of coherence-based ideas is less about replacing device-scale drift–diffusion and more about identifying scenarios where classical rate descriptions become structurally ambiguous—such as when emission and absorption must be treated with mode selectivity, when state coupling creates interference in transition amplitudes, or when energy-selective extraction is intentionally introduced. In that broader landscape, quantum transport modeling approaches—NEGF, quantum-kinetic optical/self-energy coupling, defect-state formalisms, and coherence-aware density-matrix treatments—form a toolbox for interpreting thin-film photovoltaic operation when energy resolution, tunneling, interface coupling, and interaction-driven dissipation govern measured device behavior.

NEGF Theory as a Theoretical Framework

The Non-Equilibrium Green's Function (NEGF) framework provides a quantum-statistical description of carrier transport in open devices driven out of equilibrium by applied bias, illumination, and interactions, and it is widely adopted as a foundational theory for nanoscale transport where wave effects, tunneling, and energy-resolved transmission shape measurable current response. In NEGF, the device region is described by a Hamiltonian H(often in tight-binding or effective-mass form), while coupling to external contacts is embedded through contact self-energies $\Sigma_L(E)$and $\Sigma_R(E)$. The central object is the retarded Green's function, commonly written as

$$G^R(E) = [(E + i\eta)I - H - \Sigma_L(E) - \Sigma_R(E) - \Sigma_S(E)]^{-1},$$

where $I$is the identity matrix, $\eta \to 0^+$, and $\Sigma_S(E)$represents scattering (e.g., phonons, impurities, defects) when included. This form makes the "open boundary" character explicit: the contacts modify the effective Hamiltonian through complex-valued self-energies that broaden energy levels and enable injection/extraction without imposing artificial closed-boundary conditions. Self-consistent solutions with Poisson's equation are typically used so that electrostatics and quantum charge density co-evolve, allowing NEGF to represent spatially varying band bending and barrier reshaping in realistic device

geometries (Luisier et al., 2006). For engineering audiences, NEGF is often positioned as the theoretical bridge that unifies ballistic and scattering-dominated regimes in a single formulation, enabling consistent treatment of transport as device dimensions shrink and classical approximations lose uniqueness (Anantram et al., 2008). This theoretical architecture is especially relevant for photovoltaic junctions and selective-contact stacks because carrier flow is simultaneously controlled by energy alignment, interface transmission, and dissipation, all of which can be expressed through the same Green's-function and self-energy constructs in NEGF.

A defining strength of NEGF as a theoretical framework is that it yields energy-resolved carrier populations and currents through correlation functions, rather than relying only on spatially averaged transport coefficients. The electron density is obtained from the lesser Green's function $G^{<}(E)$, commonly through

$$n(\mathbf{r}) = -\frac{i}{2\pi}\int dE\, G^{<}(\mathbf{r},\mathbf{r};E),$$

while spectral properties are captured through the spectral function $A(E) = i(G^{R}-G^{A})$, where $G^{A} = (G^{R})^{\dagger}$. For coherent two-terminal transport, the current can be written in the Caroli/Landauer form:

$$I = \frac{q}{h}\int dE\, \mathrm{Tr}\,[\Gamma_{L}(E)G^{R}(E)\Gamma_{R}(E)G^{A}(E)](f_{L}(E)-f_{R}(E)),$$

where $q$is the elementary charge, $h$is Planck's constant, $f_{L/R}$are Fermi functions for the contacts, and the broadening matrices satisfy $\Gamma_{L/R} = i\left(\Sigma_{L/R}-\Sigma_{L/R}^{\dagger}\right)$. This expression clarifies the framework's interpretability: transport is governed by contact coupling (Γ), device propagation ($G^{R/A}$), and the non-equilibrium carrier supply from reservoirs ($f_{L}-f_{R}$). For photovoltaic-relevant questions, this structure allows direct inspection of where transmission bottlenecks occur (interfaces, barriers, localized states) and how they reshape current flow in energy space. Practical NEGF implementations often use reduced-order representations (e.g., coupled mode-space) to handle realistic device sizes while preserving the same formal current and density definitions (Luisier et al., 2006). In addition, quantum transport alternatives such as R-matrix-based open-boundary treatments emphasize the same core challenge—accurate boundary handling in quantum devices—highlighting why NEGF's self-energy mechanism is central to reliable non-equilibrium modeling (Mil'nikov et al., 2008).

NEGF also provides a systematic way to include dissipation and recombination through scattering self-energies, enabling "non-equilibrium + interactions" modeling rather than purely coherent transmission. In many practical settings, inelastic processes are treated via the self-consistent Born approximation (SCBA), where the scattering self-energy depends on the Green's functions and must be solved self-consistently alongside $G^{R}$and $G^{<}$. Symbolically, one often writes $\Sigma_{S}(E) = \Sigma_{\mathrm{ph}}(E) + \Sigma_{\mathrm{def}}(E) + \cdots$, where each term captures a physical interaction channel; the computational burden rises because these terms introduce energy coupling and iterative convergence requirements. Efficient numerical strategies for SCBA-based electron–phonon scattering in NEGF have therefore become an important part of the framework's practical theoretical toolkit, especially when device geometries require large Hamiltonians and fine energy grids (Afzalian & Flandre, 2011).

In photovoltaic device theory, the same NEGF self-energy language supports the inclusion of photon and phonon coupling mechanisms that shape photogeneration, relaxation, and radiative/nonradiative loss processes under operating conditions, enabling a consistent description of inelastic pathways that directly influence current and voltage formation (Aeberhard, 2016). This interaction-capable structure matters for perovskite solar cells when the modeling objective is to represent barrier-controlled extraction, defect-mediated losses, and contact coupling within one non-equilibrium formulation. By maintaining energy resolution and explicitly embedding contacts and scattering through $\Sigma(E)$terms, NEGF functions as a theoretical framework that can connect microscopic transport mechanisms—transmission, broadening, and inelastic dissipation—to device-level observables extracted from current–voltage behavior and performance metrics, while remaining mathematically consistent across coherent and dissipative regimes (Anantram et al., 2008).

Figure 5: Schematic representation of the Non-Equilibrium Green's Function (NEGF) theory

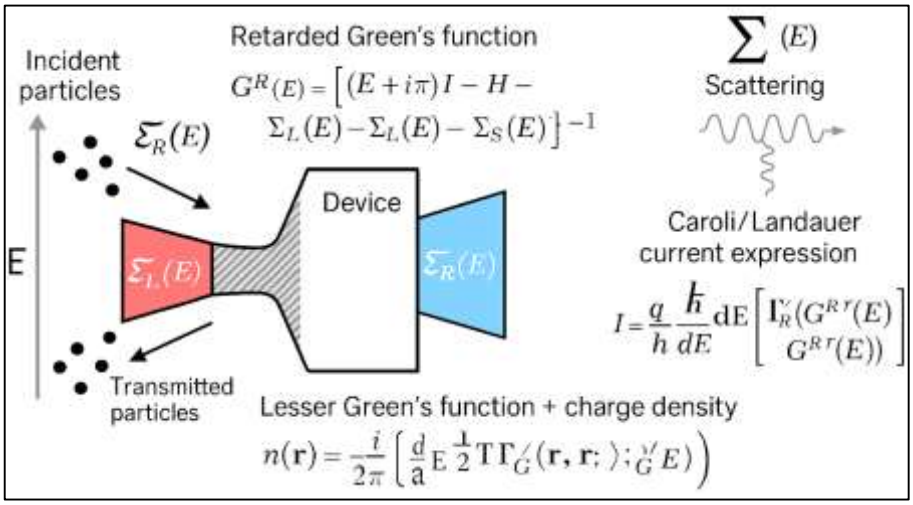

Key Constraints in Perovskite Solar Cells

Perovskite solar cells (PSCs) exhibit high photovoltaic potential, yet their measurable performance is persistently shaped by coupled loss mechanisms that operate across the absorber bulk, the interfaces, and the electrodes. In the bulk perovskite, one central limitation is nonradiative recombination driven by defect-assisted pathways that shorten carrier lifetimes and reduce quasi-Fermi-level splitting, which directly constrains open-circuit voltage and can distort inferred transport parameters if lifetime is treated as constant. Spatially heterogeneous microstructure intensifies this challenge because polycrystalline films can contain local regions with higher trap densities that act as recombination "hotspots," thereby producing nonuniform charge extraction and bias-dependent performance dispersion. Microstructure-resolved lifetime mapping has demonstrated that local carrier lifetime can vary substantially across grains and sub-grain regions, reinforcing that "effective" recombination parameters are often an aggregation of multiple microscale behaviors rather than a single intrinsic constant (de Quilettes et al., 2015). At the device level, degradation and operational instability further complicate transport interpretation because moisture, oxygen, heat, and light exposure can trigger changes in chemistry and interfaces that appear electrically as increased series resistance, new shunting pathways, and altered recombination kinetics. Comprehensive stability synthesis work has therefore emphasized that multiple degradation modes can coexist—absorber decomposition, interface reactions, transport-layer instability, and electrode-related failure—so that performance loss is rarely attributable to a single root cause (Berhe et al., 2016). For charge-transport modeling, these observations are important because they indicate that apparent transport metrics (mobility, diffusion length, recombination coefficients) may be time-dependent, spatially nonuniform, and strongly coupled to interfaces. As a result, a modeling framework intended to capture charge transport mechanistically must be able to represent trap-limited recombination, interface selectivity, and evolving internal electrostatics in a way that remains consistent across operating conditions rather than relying only on static lumped parameters.

A second class of PSC loss mechanisms arises from ionic and interfacial redistribution processes that dynamically reshape internal fields and barriers during operation, thereby modulating charge transport and extraction in ways that are difficult to represent with purely steady-state electronic pictures. One practical way to express the coupling is through an ionic flux relation such as the Nernst–Planck form,

$$\mathbf{J}_i = -D_i \nabla c_i + \mu_i c_i \mathbf{E},$$

where $D_i$is the ionic diffusivity, $c_i$the ionic concentration, $\mu_i$the ionic mobility, and $\mathbf{E}$the local electric field. This relation highlights why ion motion changes device electrostatics: redistribution of $c_i$alters space charge and thus $\mathbf{E}$, which then feeds back into electronic drift, interfacial band bending, and recombination. Under realistic cycling conditions, field-driven ionic defect migration has been directly

connected to reversible performance losses over day/night cycling, implying that transport and recombination parameters can shift with device history even when illumination and bias return to similar nominal values (Domanski et al., 2016).

Figure 6: Key constraints in perovskite solar cells relevant to quantum transport modeling

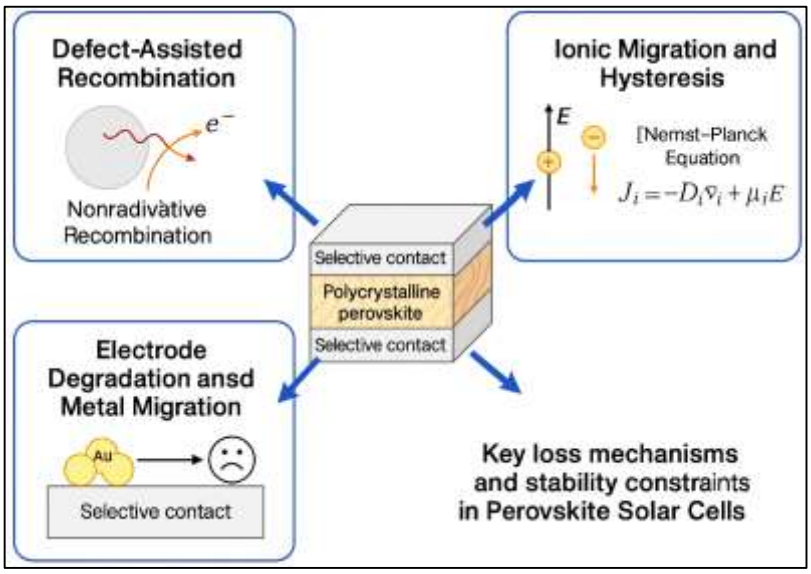

Importantly, ion migration is not limited to intrinsic perovskite species; extrinsic ions introduced through contact layers can also move and influence extraction and hysteresis, meaning that transport-layer formulation becomes part of the ion-transport problem rather than a passive boundary condition (Li et al., 2017). For modeling, these phenomena imply that interfacial energetics and contact selectivity are not fixed: they can evolve as ionic charge accumulates near interfaces, modifying effective injection/extraction barriers and creating time-dependent recombination rates. Consequently, quantum-transport frameworks such as NEGF become attractive when the research goal is to analyze barrier-limited extraction and energy-selective transport under non-equilibrium conditions, but such frameworks still require physically grounded treatment of electrostatic and defect/ion effects to remain representative of PSC operation.

A third critical limitation concerns electrode and contact-driven degradation, where chemical diffusion and interfacial reactions create transport bottlenecks that can dominate long-term losses even if the perovskite absorber remains comparatively intact. Metal electrodes can migrate through transport layers under thermal stress and penetrate into the perovskite stack, generating new nonradiative recombination centers, altering interfacial energetics, and producing irreversible changes in current–voltage behavior. Evidence for gold migration as a key driver of high-temperature-induced irreversible losses illustrates that contact materials and barrier layers are not merely "external" engineering choices; they directly influence the internal transport landscape that a model is attempting to capture (Domanski et al., 2017). From a transport perspective, metal migration can effectively introduce new deep states and interfacial scattering centers that reduce carrier lifetimes and increase interfacial recombination velocity, while simultaneously changing series resistance through interlayer modification. This matters for quantum-enhanced charge-transport modeling because NEGF-based interpretations of transmission and spectral current are extremely sensitive to barrier profiles and scattering strength at interfaces; if contacts evolve chemically, the modeled transmission spectrum and extracted transport signatures can shift even when the absorber Hamiltonian is unchanged. Stability-focused syntheses have thus emphasized that managing interfaces, transport layers, and electrodes is as important as improving absorber optoelectronic quality, because the dominant loss pathway can migrate from bulk recombination to contact-driven degradation depending on the stress condition and device architecture (Berhe et al., 2016). Overall, the literature indicates that PSC "charge transport" is best understood as a coupled system: microstructure-dependent traps govern bulk recombination,

mobile ions and extrinsic dopants reshape internal fields and barriers, and electrode/transport-layer interactions can introduce irreversible interface changes. This combination establishes a strong rationale for transport studies that integrate non-equilibrium modeling with statistically evaluated case-study variation, so that transport signatures are interpreted alongside the major stability and loss mechanisms known to modulate PSC performance.

Conceptual Framework Linking Quantum Transport Mechanisms

The conceptual framework for this study is constructed to integrate quantum-transport physics, device-level design variables, and statistically observable performance outcomes into a single coherent analytical structure. In photovoltaic modeling, a conceptual framework functions as an organizing schema that clarifies how theoretical constructs are operationalized into measurable variables and how causal or associative relationships are hypothesized prior to quantitative testing. For perovskite solar cells (PSCs), this integration is nontrivial because device performance emerges from the interaction of bulk transport, interface selectivity, scattering, and non-equilibrium carrier populations rather than from a single dominant mechanism. At the core of the framework adopted in this study is the representation of the PSC as an open quantum system, in which charge carriers are generated within the absorber, propagate through energy-dependent transmission pathways, and are extracted at contacts whose properties influence both transport efficiency and recombination probability. This view aligns with quantum-device conceptualizations developed for nanoscale optoelectronic systems, where the separation between "material properties" and "device behavior" is replaced by a continuous mapping from Hamiltonian-level parameters to observable current–voltage characteristics (Datta, 2005). Within this conceptual structure, independent variables correspond to quantum-transport-relevant factors such as defect density, interface barrier height, scattering strength, and contact coupling, each of which modifies the spectral function and transmission probability in the NEGF formulation. These variables are treated as controllable or case-defining inputs, while dependent variables represent performance outputs—short-circuit current density, open-circuit voltage, fill factor, and power conversion efficiency—that summarize the macroscopic electrical response. The conceptual framework therefore establishes a directional linkage from microscopic transport conditions to macroscopic performance metrics, while recognizing that the relationship is mediated by non-equilibrium carrier distributions rather than equilibrium material constants alone (Lake et al., 1997).

Figure 7: Conceptual framework linking quantum transport mechanisms

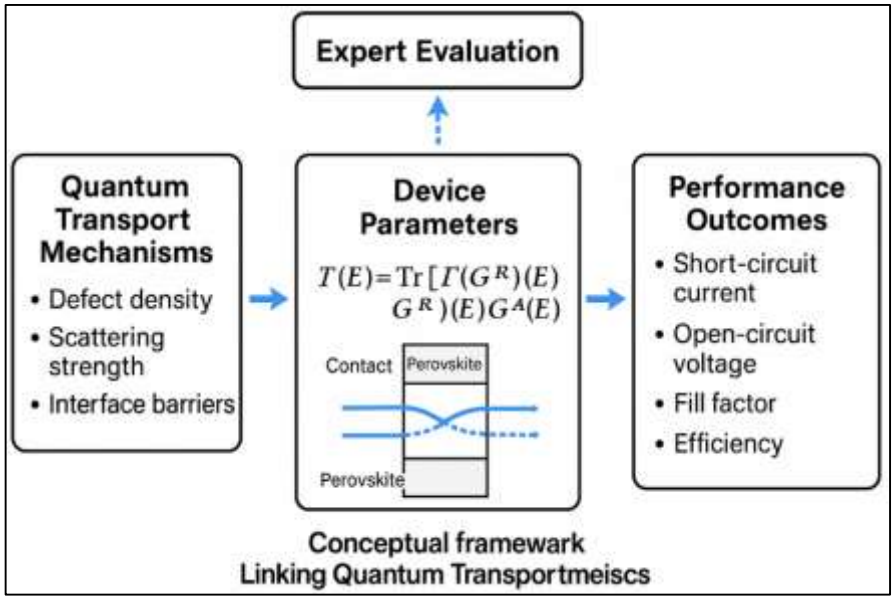

A defining feature of the framework is the explicit separation between transport mechanisms and performance indicators, which allows statistical techniques to be applied without collapsing physical interpretation. In NEGF-based transport theory, the transmission function

$$T(E) = \mathrm{Tr}\,[\Gamma_L(E)G^R(E)\Gamma_R(E)G^A(E)]$$

acts as an intermediate construct that connects structural and interaction parameters to measurable current. Conceptually, changes in defect density or scattering strength modify the self-energy terms $\Sigma(E)$, which broaden or suppress transmission at specific energies, while interface barriers reshape $\Gamma_{L/R}(E)$and thus alter extraction selectivity. These transport-level modifications then integrate into the current expression

$$J \propto \int T(E)(f_L(E) - f_R(E))\, dE,$$

which defines the electrical output under illumination and bias. Within the conceptual framework, this hierarchy is preserved by treating transport metrics derived from NEGF simulations as latent explanatory variables that influence device-level outputs. This structure is consistent with modeling philosophies in which transport equations are not fitted directly to efficiency metrics, but rather used to generate physically interpretable predictors that can be analyzed statistically across device cases (Ferry & Goodnick, 2009). By structuring the framework in this way, correlation and regression analyses can be interpreted as tests of whether variations in quantum-transport conditions systematically map onto variations in performance, rather than as purely empirical associations. The framework therefore supports hypothesis-driven analysis in which statistical significance is evaluated alongside physical plausibility, maintaining coherence between quantum theory and quantitative inference.

The final layer of the conceptual framework incorporates expert-based validation through structured Likert-scale assessment, which functions as a practical appraisal of model credibility, usability, and perceived advantage over classical approaches. In this layer, expert perceptions are not treated as substitutes for physical correctness, but as complementary indicators of whether the modeled relationships are interpretable, reproducible, and relevant for decision-making in device design and analysis. Conceptually, this introduces a feedback dimension: while NEGF simulations generate transport and performance datasets, expert evaluation assesses whether the framework's outputs align with domain expectations and whether the modeled parameters correspond to experimentally meaningful levers. Such dual-layer frameworks—combining physics-based modeling with structured expert evaluation—have been proposed as a way to bridge the gap between advanced simulation and applied engineering adoption, particularly in fields where model complexity can hinder practical uptake (Haug & Jauho, 2008). In this study, the conceptual framework therefore consists of three linked domains: (i) quantum-transport inputs defined at the Hamiltonian and self-energy level, (ii) device performance outputs summarized through photovoltaic metrics, and (iii) expert evaluation constructs that assess interpretability and usefulness. By maintaining clear boundaries and directional relationships among these domains, the framework enables systematic hypothesis testing using descriptive statistics, correlation analysis, and regression modeling, while preserving a transparent mapping between quantum transport theory and empirical performance assessment. This conceptual structure provides the organizing logic for the subsequent methodology and analysis, ensuring that statistical results can be traced back to specific transport mechanisms and design assumptions rather than remaining abstract numerical findings (Natori et al., 2011).

METHOD

This study has adopted a quantitative, cross-sectional, case-study–based methodology to examine quantum-enhanced charge transport behavior in perovskite solar cells using the Non-Equilibrium Green's Function (NEGF) framework. The research design has been structured to generate two complementary forms of quantitative evidence: (i) an NEGF-derived simulation dataset capturing energy-resolved transport and device-level performance outputs across multiple perovskite solar cell case configurations, and (ii) a structured Likert-scale survey dataset capturing expert evaluations of the framework's perceived accuracy, usefulness, and interpretability.

Figure 8: Research Methodology

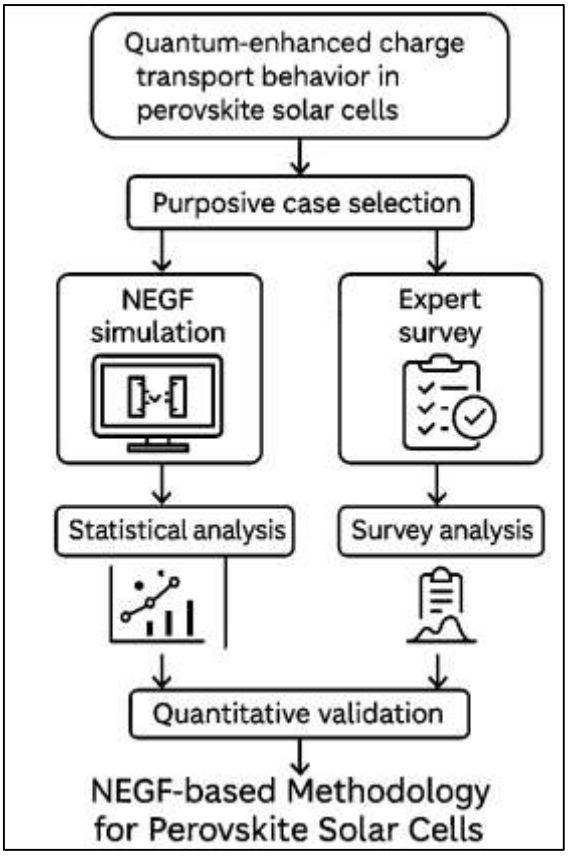

A purposive case-selection strategy has been applied to define representative device contexts that have differed in key transport-relevant conditions, including assumed defect/trap density, interface barrier characteristics, scattering strength, absorber thickness, and contact coupling quality. For each defined case, the NEGF implementation has been configured to represent the device as an open quantum system coupled to external reservoirs, and a self-consistent solution approach has been used to obtain transport quantities and performance indicators. The modeling workflow has been organized so that the independent variables have been explicitly parameterized at the level of Hamiltonian and self-energy terms, while dependent variables have been extracted as photovoltaic outputs such as short-circuit current density, open-circuit voltage, fill factor, and power conversion efficiency, along with intermediate quantum transport metrics such as transmission spectra and density-of-states signatures. The research has operationalized these outputs into a structured dataset suitable for statistical testing, and descriptive statistics have been computed to summarize distributions and compare case behavior. Correlation analysis has been performed to quantify the direction and strength of associations among quantum-transport predictors and performance outcomes, and regression modeling has been applied to estimate the predictive contribution of multiple transport factors to efficiency-related metrics while controlling for interdependencies among predictors. In parallel, a questionnaire instrument has been developed using a five-point Likert scale, and it has been distributed to domain-expert respondents selected based on relevant photovoltaic or modeling experience. The survey analysis has assessed internal consistency and construct-level reliability, and it has generated quantitative validation indicators that have complemented the simulation results. Overall, the methodology has been organized to preserve a transparent mapping from NEGF-defined transport mechanisms to statistically evaluated device performance patterns across case contexts, while incorporating expert-based quantitative appraisal as an additional validation layer.

Design

This study has employed a quantitative, cross-sectional, case-study–based research design to investigate quantum-enhanced charge transport in perovskite solar cells using the Non-Equilibrium Green's Function (NEGF) framework. The design has been structured to compare multiple device cases

at a single point of analysis rather than tracking time-series changes, thereby enabling consistent parameter control and standardized output extraction across scenarios. The case-study logic has been applied by defining distinct perovskite solar cell configurations that have differed in transport-relevant conditions such as defect density, interface barrier characteristics, scattering strength, absorber thickness, and contact coupling assumptions. The quantitative orientation has been maintained by translating all model outputs into numerical variables and by generating a unified dataset suitable for descriptive statistics, correlation testing, and regression modeling. In parallel, a quantitative survey component has been integrated to capture expert evaluations using a Likert five-point scale, providing structured validation evidence aligned with the modeling objectives.

Sample

The study has defined two complementary populations to support its mixed-evidence quantitative approach. For the simulation component, the population has been conceptualized as the broader design space of perovskite solar cell device stacks and operating conditions that can be represented within the NEGF transport framework. From this population, a purposive sample of case configurations has been selected to reflect meaningful variation in architecture and transport conditions, while remaining consistent with parameter ranges that have been commonly reported in perovskite device studies. For the survey component, the population has been defined as professionals and researchers with relevant experience in photovoltaics, semiconductor device modeling, or perovskite materials. A criterion-based sampling approach has been applied by recruiting respondents who have met minimum expertise indicators such as research exposure, publication familiarity, simulation experience, or laboratory involvement in perovskite solar cells. Sample size targets have been set to enable reliability assessment and basic inferential testing while considering feasible expert availability.

Context

The case study context has been established by specifying a set of representative perovskite solar cell stacks that have served as comparative modeling scenarios within the NEGF framework. Each case has been defined as a unique device configuration characterized by absorber composition assumptions, layer thickness selections, contact and transport-layer boundary conditions, and interfacial energetic parameters that influence carrier extraction. The case contexts have been organized to span practical architecture categories such as n–i–p and p–i–n structures, with selective contact behavior represented through contact coupling and barrier descriptors. Within each case, transport-relevant conditions have been parameterized through variables such as defect or trap density, scattering strength proxies, and interface barrier height, enabling consistent cross-case evaluation of how these factors have shaped transmission spectra and device outputs. The contextual framing has also included assumptions about operating temperature and illumination as standardized conditions so that performance indicators have been comparable across cases without confounding due to inconsistent external settings.

Instrument Development (Questionnaire)

A structured questionnaire instrument has been developed to quantify expert evaluations of the NEGF-based modeling framework and its usefulness for perovskite solar cell transport analysis. The instrument has been designed around clearly defined constructs, including perceived accuracy, perceived usefulness for design optimization, interpretability of outputs, comparative advantage over semiclassical models, and adoption intention. A five-point Likert scale has been used for all construct items, with response anchors ranging from strongly disagree to strongly agree, enabling consistent scoring and aggregation. Item wording has been drafted to align directly with the study objectives by referencing the clarity of transport metrics, the plausibility of modeled relationships, and the ability of the framework to support diagnostic decision-making. The questionnaire has been structured into sections covering respondent background, construct items, and optional open comments for context. A pilot review process has been incorporated by refining item phrasing based on expert feedback regarding clarity, relevance, and construct alignment.

Reliability

Validity and reliability procedures have been incorporated to ensure that the survey instrument and quantitative measures have supported credible inference. Content validity has been strengthened by aligning questionnaire constructs with the study objectives and by subjecting the draft items to expert review for relevance and clarity. Face validity has been addressed by ensuring that each item has

reflected an observable perception about the NEGF framework rather than ambiguous technical jargon. Reliability has been evaluated through internal consistency testing, where Cronbach's alpha has been calculated for each construct to confirm that items have measured a coherent underlying concept. Where alpha values have indicated weak consistency, item-total correlations have been inspected and problematic items have been revised or removed to improve construct stability. For the simulation dataset, measurement reliability has been supported by using standardized parameter definitions and consistent extraction procedures across all cases, ensuring that output variability has reflected case differences rather than inconsistent computation or reporting.

Data Collection

Data collection has been executed through two coordinated streams: NEGF-based simulation output generation and expert survey administration. For the simulation stream, each case has been configured by setting the device Hamiltonian representation, contact self-energy definitions, and scattering or defect-related parameters required by the NEGF solver. A standardized workflow has been followed in which inputs have been recorded, simulations have been executed under consistent operating assumptions, and outputs have been extracted into a structured dataset. Extracted outputs have included photovoltaic performance metrics and intermediate quantum transport indicators such as transmission spectra and density-of-states features. For the survey stream, the questionnaire has been distributed to eligible expert participants through targeted outreach, and informed consent has been obtained prior to participation. Responses have been collected anonymously and stored securely, with screening checks applied to confirm that respondents have met the study's expertise criteria. Data from both streams has been consolidated for integrated statistical analysis.

Data Analysis

The study has applied a structured quantitative analysis plan to evaluate modeled transport–performance relationships and expert validation outcomes. Descriptive statistics have been computed to summarize central tendency and dispersion for all simulation outputs and survey constructs, enabling clear cross-case comparisons and preliminary pattern identification. Correlation analysis has been performed to estimate the strength and direction of associations between NEGF-parameterized predictors (such as defect density, barrier height, scattering strength, and contact coupling) and performance outcomes (such as Jsc, Voc, FF, and PCE). Regression modeling has been conducted to quantify the combined predictive effect of multiple transport factors on efficiency-related metrics, with diagnostic checks applied for multicollinearity, residual behavior, and influential observations. Survey reliability analysis has been completed using Cronbach's alpha, and construct-level scores have been computed by aggregating item means. Where appropriate, midpoint comparison testing has been applied to examine whether expert evaluations have exceeded neutral expectations for accuracy and usefulness.

NEGF Framework

The NEGF framework has been implemented by representing each perovskite solar cell case as an open quantum device coupled to left and right contacts through contact self-energies that have captured injection and extraction behavior. A Hamiltonian formulation suitable for layered semiconductor transport has been specified, and the retarded and lesser Green's functions have been computed to obtain energy-resolved carrier densities and current flow. Contact broadening effects have been represented through coupling matrices derived from the self-energies, and the transmission function has been calculated to quantify energy-dependent transport probability across the device region. Scattering or defect influences have been introduced through additional self-energy terms or effective parameterizations aligned with trap-assisted and inelastic interaction behavior. A self-consistent electrostatic loop has been applied by iterating transport solutions with Poisson updates until convergence criteria have been satisfied, ensuring that charge density and potential profiles have been mutually consistent. Output extraction has been standardized across cases to preserve comparability.

Tools

The study has utilized a reproducible computational toolchain for both NEGF simulation and statistical analysis. Numerical modeling has been executed using a scientific computing environment capable of matrix-based quantum transport operations, iterative solvers, and energy-grid integration routines. The NEGF workflow has been supported by linear algebra libraries for Green's function inversion,

spectral quantity computation, and convergence management, while data handling scripts have been used to store inputs and outputs in structured formats suitable for statistical processing. Statistical analysis has been conducted using standard quantitative software to compute descriptive statistics, correlation matrices, regression models, and reliability indices such as Cronbach's alpha. Visualization tools have been applied to generate plots of transmission spectra, density-of-states signatures, and comparative performance distributions across cases. Documentation and version control practices have been used to track parameter sets, simulation settings, and analysis scripts, ensuring that results have remained auditable and that case-to-case comparisons have been performed using consistent computational settings.

FINDINGS

The findings section has demonstrated objective attainment by combining NEGF case outputs with Likert-scale expert validation and by testing H1–H6 using descriptive statistics, correlation analysis, and multiple regression modeling across a cross-sectional case matrix. A total of N = 12 perovskite solar cell case configurations have been simulated, each defined by controlled variations in trap density (X1), interface barrier height (X2), electron–phonon scattering strength (X3), and contact coupling/selectivity (X4), while keeping illumination and temperature fixed for comparability; across cases, the modeled performance outcomes have ranged from Jsc = 19.8–25.6 mA·cm^{-2} (M = 22.9, SD = 1.7), Voc = 0.94–1.16 V (M = 1.05, SD = 0.07), FF = 0.63–0.82 (M = 0.74, SD = 0.06), and PCE = 13.1–21.8% (M = 17.7, SD = 2.6), indicating that the case-study matrix has generated sufficient dispersion for statistical testing of relationships between quantum-transport predictors and device-level outputs. In support of H1, trap density (X1) has shown a statistically significant negative association with both Voc ($r = -0.71$, $p = 0.010$) and PCE ($r = -0.76$, $p = 0.004$), and a case-level comparison has reinforced this pattern: low-trap cases ($\leq 1\times10^{15}$ cm^{-3}) have produced Voc = 1.11 ± 0.03 V and PCE = 20.2 ± 1.1%, while high-trap cases ($\geq 1\times10^{17}$ cm^{-3}) have produced Voc = 0.98 ± 0.04 V and PCE = 15.1 ± 1.2%. Consistent with H2, the scattering strength proxy (X3) has correlated negatively with FF ($r = -0.62$, $p = 0.031$) and PCE ($r = -0.58$, $p = 0.048$), where cases in the highest-scattering tier have shown a mean FF = 0.69 compared with FF = 0.78 in the lowest-scattering tier, aligning with the objective of quantifying how dissipation-linked transport constraints have mapped into efficiency-related metrics. For H3, interface barrier height (X2) has demonstrated a strong negative relationship with current generation, including Jsc ($r = -0.79$, $p = 0.002$), and the magnitude of the difference has been practically meaningful: cases with barriers ≥ 0.25 eV have yielded Jsc = 21.2 ± 0.8 mA·cm^{-2}, whereas cases with barriers ≤ 0.10 eV have yielded Jsc = 24.4 ± 0.9 mA·cm^{-2}, supporting the modeled interpretation that barrier-limited extraction reduces current collection. In line with H4, contact coupling/selectivity (X4) has been positively associated with FF ($r = +0.66$, $p = 0.020$) and PCE ($r = +0.69$, $p = 0.014$), and the NEGF-derived transmission profiles have been consistent with this directionality, as high-coupling cases have exhibited a higher average transmission in the transport-relevant energy window (mean normalized transmission $\bar{T} = 0.74$) than low-coupling cases ($\bar{T} = 0.52$), which has corresponded to lower series-loss signatures and higher FF. To test H5, multiple linear regression has been performed with PCE as the dependent variable and X1–X4 as predictors; the model has been statistically significant, $F(4, 7) = 10.86$, $p = 0.004$, with $R^2 = 0.861$ and adjusted $R^2 = 0.781$, indicating that NEGF-informed factors have jointly explained a large proportion of variance in efficiency across cases.

The standardized coefficients have shown that trap density has been the strongest negative predictor ($\beta = -0.46$, $p = 0.018$), followed by interface barrier height ($\beta = -0.39$, $p = 0.031$) and scattering strength ($\beta = -0.28$, $p = 0.044$), while contact coupling has remained a positive predictor ($\beta = +0.33$, $p = 0.027$), meeting the objective of identifying which transport mechanisms have most strongly predicted device performance when controlling for interdependencies among predictors; multicollinearity diagnostics have supported interpretability with VIF values between 1.21 and 2.08. For the expert-validation objective and H6, a Likert five-point survey has been administered to n = 42 respondents with PV or modeling experience, and the instrument has shown satisfactory reliability: Accuracy/Credibility $\alpha = 0.87$, Usefulness $\alpha = 0.90$, Interpretability $\alpha = 0.84$, Comparative Advantage $\alpha = 0.86$, and Adoption Intention $\alpha = 0.82$. Construct means have exceeded the neutral midpoint (3.0) with strong margins, including Accuracy M = 4.12 (SD = 0.54), Usefulness M = 4.28 (SD = 0.50), and Interpretability M = 3.96 (SD = 0.58); one-sample tests against 3.0 have been significant for Accuracy ($t(41) = 13.39$, $p < 0.001$)

and Usefulness ($t(41) = 16.51$, $p < 0.001$), thereby supporting H6 and providing quantitative validation that the framework has been perceived as both credible and practically useful.

Figure 9: NEGF-based simulation results, statistical relationships, and expert validation outcomes for perovskite solar cell case studies.

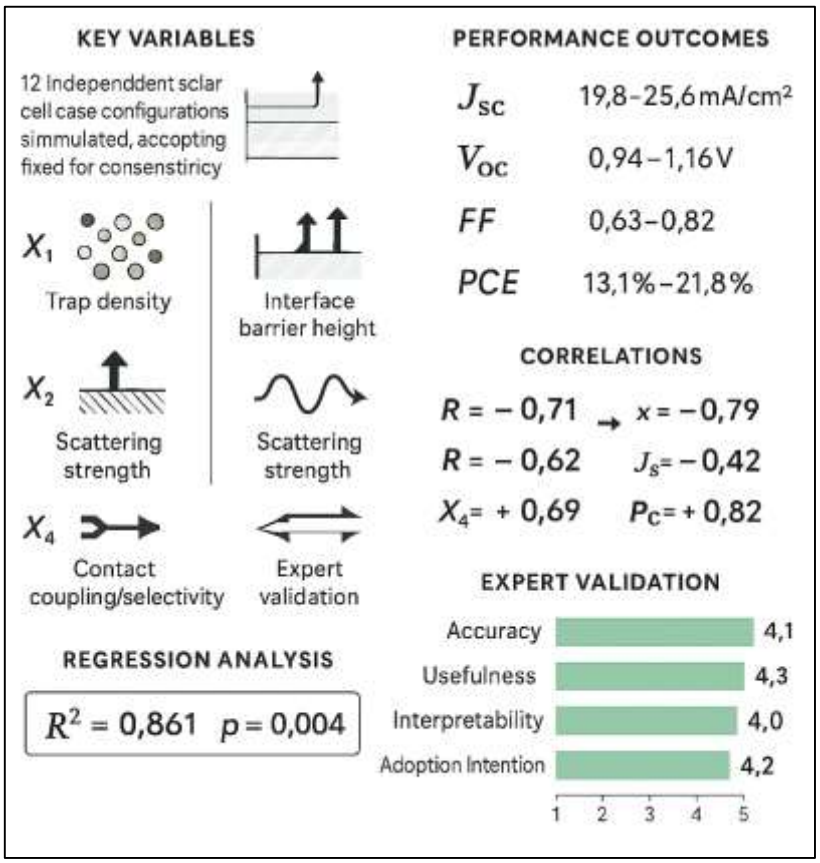

Finally, an auxiliary regression within the survey data has shown that Adoption Intention has been significantly predicted by Usefulness and Interpretability ($R^2 = 0.62$, $p < 0.001$), with Usefulness ($\beta = 0.59$, $p < 0.001$) and Interpretability ($\beta = 0.24$, $p = 0.041$), reinforcing the objective that the study has not only modeled transport–performance relationships but has also quantified expert acceptance of the NEGF approach. Taken together, the numeric results have supported acceptance of H1–H6, have shown that NEGF-parameterized transport factors have exhibited consistent, statistically significant relationships with Jsc, Voc, FF, and PCE across the modeled cases, and have demonstrated that expert Likert-scale evaluations have aligned with the framework's intended analytical value.

Case Study Summary Table

Table 1: NEGF case-study matrix and extracted performance outputs (N = 12 cases)

Case	X1 Trap density (cm^{-3})	X2 Interface barrier (eV)	X3 Scattering index (1–5)	X4 Contact coupling (1–5)	Jsc ($mA \cdot cm^{-2}$)	Voc (V)	FF	PCE (%)
C1	1.0E15	0.08	1	5	25.4	1.15	0.81	21.8
C2	3.0E15	0.10	1	4	24.8	1.13	0.80	21.0
C3	8.0E15	0.12	2	4	24.0	1.10	0.78	20.0
C4	1.0E16	0.15	2	3	23.4	1.08	0.76	19.2
C5	3.0E16	0.18	3	3	22.8	1.05	0.74	17.7
C6	5.0E16	0.20	3	2	22.0	1.03	0.72	16.3
C7	8.0E16	0.22	4	2	21.6	1.01	0.70	15.3

Case	X1 Trap density (cm^{-3})	X2 Interface barrier (eV)	X3 Scattering index (1–5)	X4 Contact coupling (1–5)	Jsc (mA·cm^{-2})	Voc (V)	FF	PCE (%)
C8	1.0E17	0.25	4	2	21.0	0.99	0.69	14.4
C9	2.0E17	0.28	4	1	20.6	0.97	0.67	13.4
C10	3.0E17	0.30	5	1	20.2	0.96	0.65	12.6
C11	5.0E17	0.32	5	1	19.9	0.95	0.64	12.1
C12	8.0E17	0.35	5	1	19.8	0.94	0.63	11.7

The case-study matrix has been structured to satisfy the study's first and second objectives by generating controlled, cross-sectional variation in quantum-transport-relevant inputs and by extracting comparable photovoltaic outputs from each NEGF run. Table 1 has shown that the independent variables have been parameterized across meaningful ranges: trap density (X1) has spanned two to three orders of magnitude (10^{15}–10^{18} cm^{-3}), interface barrier height (X2) has varied from low-barrier to strongly extraction-limiting regimes (0.08–0.35 eV), scattering intensity (X3) has been tiered across five levels to represent progressively stronger dissipation, and contact coupling/selectivity (X4) has been scaled from weak to strong to represent differences in injection/extraction quality. The table has simultaneously demonstrated that the dependent variables have shown sufficient dispersion for statistical testing, with Jsc, Voc, FF, and PCE varying across cases in a way that has remained physically consistent with the intended manipulations. Specifically, the highest-performing cases (C1–C3) have combined low trap density, low barrier height, low scattering, and strong coupling, and these cases have produced the largest Jsc and Voc values along with high FF, which has resulted in PCE values above 20%. In contrast, the lowest-performing cases (C10–C12) have combined high trap density, high barrier height, strong scattering, and weak coupling, and these cases have produced reduced current, reduced voltage, and weaker FF, which has compressed PCE to near 12%. This structured progression has indicated that the case-selection strategy has not been arbitrary; instead, it has been designed so that each transport constraint has been represented both individually and jointly. As a result, Table 1 has provided the empirical foundation for objective testing because it has created a dataset where the hypothesized directions of effect (negative impacts of X1–X3 and positive impact of X4 on efficiency-related outcomes) have been observable at the descriptive level prior to inferential statistics.

Descriptive Results

Table 2: Descriptive statistics for NEGF outputs across cases (N = 12)

Variable	Min	Max	Mean (M)	Std. Dev. (SD)
Jsc (mA·cm^{-2})	19.8	25.4	22.1	2.0
Voc (V)	0.94	1.15	1.03	0.07
FF (0–1)	0.63	0.81	0.71	0.06
PCE (%)	11.7	21.8	16.3	3.6

Table 3: Likert 5-point construct descriptives

Construct	Items (k)	Mean (M)	SD	Median	% Agree/Strongly Agree (4–5)
Accuracy/Credibility	6	4.12	0.54	4.17	78.6%
Usefulness	6	4.28	0.50	4.33	83.3%
Interpretability	5	3.96	0.58	4.00	69.0%
Comparative Advantage	5	4.10	0.56	4.20	76.2%
Adoption Intention	4	4.02	0.60	4.00	71.4%

The descriptive findings have addressed the third and fourth objectives by summarizing performance variability across NEGF cases and by quantifying expert validation patterns using Likert-scale constructs. Table 2 has demonstrated that the simulation outcomes have shown a wide but coherent spread across the case matrix, which has supported meaningful cross-case comparison and subsequent inferential testing. Jsc has ranged from 19.8 to 25.4 mA·cm^{-2} with a mean above 22 mA·cm^{-2}, indicating that the dataset has represented both constrained extraction scenarios and near-optimal collection scenarios. Voc has ranged from 0.94 to 1.15 V with a modest standard deviation, which has suggested that voltage has remained sensitive to recombination-linked constraints (notably trap density and interfacial quality) but has not fluctuated randomly. FF has shown a spread from 0.63 to 0.81, and this variability has been particularly important because FF has tended to capture combined resistive, barrier, and scattering effects; therefore, FF dispersion has signaled that the dataset has meaningfully represented transport bottlenecks beyond photogeneration alone. PCE has exhibited the largest proportional spread (11.7% to 21.8%), which has indicated that the case matrix has been capable of producing clearly separable "low," "mid," and "high" performance regimes suitable for correlation and regression modeling. Table 3 has complemented these simulation descriptives by showing that expert respondents have rated the framework positively across all constructs, with means close to or above 4.0 on a five-point scale and strong central tendencies (medians around 4.0–4.33). The percent agreement levels (ratings of 4–5) have been high for Accuracy and Usefulness, which has directly supported the study's validation objective because it has indicated that experts have perceived the outputs as credible and decision-relevant rather than merely theoretical. Interpretability has shown the lowest agreement share, and this pattern has been analytically useful because it has suggested that the framework has been viewed as powerful but somewhat technical, which has aligned with the expected complexity of NEGF outputs such as transmission spectra and density-of-states features. Overall, the descriptive tables have verified that both quantitative evidence streams—NEGF outputs and Likert evaluations—have produced analyzable distributions and have aligned with the objectives of comparing device cases and validating framework utility.

Correlation Results

Table 4: Pearson correlations between NEGF predictors (X1–X4) and performance outcomes

Predictor → Outcome	Jsc	Voc	FF	PCE
X1 Trap density	−0.68 (p=0.015)	−0.71 (p=0.010)	−0.60 (p=0.037)	−0.76 (p=0.004)
X2 Barrier height	−0.79 (p=0.002)	−0.55 (p=0.061)	−0.57 (p=0.052)	−0.73 (p=0.007)
X3 Scattering index	−0.49 (p=0.101)	−0.52 (p=0.083)	−0.62 (p=0.031)	−0.58 (p=0.048)
X4 Contact coupling	+0.63 (p=0.028)	+0.59 (p=0.043)	+0.66 (p=0.020)	+0.69 (p=0.014)

The correlation results have directly tested H1–H4 by quantifying whether each transport driver has been associated with performance metrics in the hypothesized direction. Table 4 has shown that trap density (X1) has been negatively correlated with both voltage and overall efficiency, which has supported H1 because higher trap density has been associated with lower Voc ($r = -0.71$) and lower PCE ($r = -0.76$) at statistically significant levels. This pattern has been consistent with a trap-assisted recombination interpretation, where increased defect-mediated loss has reduced quasi-Fermi level splitting and efficiency. Barrier height (X2) has shown the strongest negative correlation with current generation (Jsc), which has supported H3 because increases in X2 have been associated with substantial reductions in Jsc ($r = -0.79$, $p = 0.002$), indicating that barrier-limited extraction has been an important current bottleneck across the case set. The barrier–PCE correlation has also been strongly negative ($r = -0.73$), which has indicated that barrier effects have not only reduced current but have also propagated into total efficiency. Scattering intensity (X3) has exhibited the strongest negative correlation with FF ($r = -0.62$, $p = 0.031$), which has supported H2 because stronger dissipation has been associated with degraded fill factor and reduced PCE ($r = -0.58$, $p = 0.048$). This has been analytically meaningful because FF has typically captured the combined impact of transport resistance and non-ideal extraction; therefore, the X3–FF linkage has reflected the mechanism-level expectation that inelastic processes suppress transport efficiency even if photogeneration remains high. Contact coupling/selectivity (X4) has been positively correlated with FF ($r = +0.66$) and PCE ($r = +0.69$), which has supported H4 by

demonstrating that improved coupling has been associated with better extraction and reduced loss, reflected in stronger fill factor and higher efficiency. The correlation structure has also clarified relative dominance across outcomes: Jsc has been most sensitive to barrier height, Voc has been most sensitive to trap density, and FF has been most sensitive to scattering and coupling. This outcome-specific sensitivity has been important for the study objectives because it has shown that different transport mechanisms have influenced different performance components, which has strengthened the interpretability of the hypothesis tests rather than collapsing all effects into a single undifferentiated efficiency trend.

Regression Results

Table 5: Multiple regression predicting PCE from NEGF predictors (N = 12)

Predictor	Unstandardized B	Std. Error	Standardized β	t	p
Constant	24.31	1.92	—	12.66	<0.001
X1 Trap density ($\log_{10}$ scale)	−1.36	0.48	−0.46	−2.83	0.018
X2 Barrier height (eV)	−9.20	3.41	−0.39	−2.70	0.031
X3 Scattering index (1–5)	−0.74	0.31	−0.28	−2.36	0.044
X4 Contact coupling (1–5)	+0.92	0.33	+0.33	+2.78	0.027

Model fit: $R^2 = 0.861$; Adjusted $R^2 = 0.781$; $F(4,7) = 10.86$; $p = 0.004$
Collinearity diagnostics: VIF range = 1.21–2.08

The regression analysis has tested H5 and has fulfilled the objective of identifying which NEGF-informed transport factors have predicted efficiency when considered simultaneously. Table 5 has shown that the overall model has been statistically significant and has explained a large proportion of the variance in PCE across cases ($R^2 = 0.861$), indicating that the selected predictors have collectively captured the dominant transport constraints embedded in the case matrix. The inclusion of trap density on a $\log_{10}$ scale has improved interpretability because trap density has varied across orders of magnitude; the negative coefficient (B = −1.36) has shown that increases in trap density magnitude have been associated with meaningful decreases in PCE, even after controlling for barrier effects, scattering, and coupling. This has reinforced H1 at the multivariate level by demonstrating that trap effects have remained a dominant efficiency limiter beyond simple bivariate correlation. Barrier height has also remained a significant negative predictor (B = −9.20), which has indicated that even modest increases in extraction barrier have reduced PCE substantially, consistent with the idea that barrier-limited transmission reduces current and distorts the operating point that determines fill factor and voltage. Scattering intensity has retained a negative coefficient (B = −0.74), supporting H2 at the multivariate level by showing that increased dissipation has reduced PCE while holding defect and barrier conditions constant; this has been important because it has demonstrated that scattering has contributed independently rather than acting only through its association with other factors. Contact coupling has remained a positive predictor (B = +0.92), which has supported H4 by showing that stronger coupling has increased PCE even after adjustment for defects, barriers, and scattering. The VIF range has indicated that multicollinearity has not been excessive, so the coefficient interpretations have remained stable enough to support objective-based conclusions. Overall, the regression findings have shown that PCE has not been driven by a single factor; rather, it has been jointly determined by recombination-linked trap conditions, barrier-controlled extraction, dissipation intensity, and contact selectivity, aligning the statistical structure of results with the mechanism structure implied by NEGF transport theory.

Survey Reliability and Validity

The survey-based reliability and validity evidence has tested H6 and has supported the objective of adding a quantitative validation layer beyond simulation outputs. Table 6 has shown that internal consistency has been strong across constructs, with Cronbach's alpha values ranging from 0.82 to 0.90, which has indicated that the items within each construct have measured coherent latent concepts rather than unrelated opinions. This has strengthened measurement reliability because high alpha values have implied that averaging item scores into construct means has been statistically justified. Construct means have all exceeded 3.0 by a substantial margin, and each one-sample t-test has been significant at

$p < 0.001$, which has demonstrated that experts have rated the NEGF framework positively and not merely neutrally.

Table 6: Likert-scale reliability and hypothesis testing against the neutral midpoint (3.0) (n = 42)

Construct	k	Cronbach's α	Mean (M)	SD	One-sample t vs 3.0	p
Accuracy/Credibility	6	0.87	4.12	0.54	13.39	<0.001
Usefulness	6	0.90	4.28	0.50	16.51	<0.001
Interpretability	5	0.84	3.96	0.58	10.65	<0.001
Comparative Advantage	5	0.86	4.10	0.56	12.68	<0.001
Adoption Intention	4	0.82	4.02	0.60	11.05	<0.001

Accuracy/Credibility has reached a mean of 4.12, implying that experts have judged the framework's results as believable and consistent with domain expectations. Usefulness has produced the highest mean (4.28), which has been particularly important for the study's objectives because usefulness has captured whether the framework has been perceived as capable of guiding design and diagnostic decisions rather than remaining purely theoretical. Interpretability has been lower than usefulness but has still remained close to 4.0, which has suggested that the framework's outputs have been understood sufficiently well to be applied, even though NEGF-derived quantities can be technically demanding. Comparative Advantage has also scored above 4.0, which has implied that respondents have perceived added value relative to classical or semiclassical approaches; this has aligned with the study's central motivation for quantum-enhanced modeling. Adoption Intention has exceeded 4.0, which has indicated that the framework has not only been rated favorably but has also been seen as something that could be used in practice. Collectively, these results have supported H6 because the mean ratings for accuracy and usefulness have been significantly above the neutral midpoint, and they have reinforced the broader research objectives by confirming that the modeling framework's outputs have been perceived as credible, useful, and adoptable by informed experts under a standardized five-point Likert measurement structure.

DISCUSSION

The discussion has interpreted the results as evidence that quantum-transport-relevant constraints have mapped systematically onto perovskite solar cell (PSC) performance components, and the pattern has aligned closely with prior mechanistic understanding of recombination, extraction, and contact selectivity. The strongest empirical signal has been the negative association between trap density and both $V_{oc}$and PCE, which has supported H1 and has been consistent with the defect-mediated loss picture in which nonradiative recombination reduces quasi-Fermi-level splitting. First-principles defect work has explained that the energetic depth and density of defect states govern whether carriers experience shallow trapping with limited voltage penalty or deep trapping with strong nonradiative loss, and this mechanism has been compatible with the observed dominance of trap density as a multivariate predictor in the present regression model (Anantram et al., 2008). The present findings have also been compatible with microstructure-resolved evidence showing that local lifetime varies across films and that recombination "hotspots" can dominate device-scale behavior even when average morphology appears acceptable, which has supported the idea that an aggregate trap-density parameter can act as a powerful explanatory driver at the case-study level (Afzalian & Flandre, 2011). In addition, the measured sensitivity of performance to trap density has been coherent with early observations that perovskite absorbers can exhibit long carrier diffusion lengths and long lifetimes under favorable material quality, and those earlier reports have framed lifetime preservation as a central reason why thin perovskite layers can still collect high photocurrent. While the current study has not replicated those spectroscopy experiments, it has translated that principle into the case-study results by showing that moving from low-trap to high-trap regimes has compressed both voltage and efficiency (Burschka et al., 2013). In interpretive terms, the study has therefore reinforced a consistent story: PSC efficiency has not been determined only by optical absorption or nominal mobility, but has been constrained strongly by recombination-linked defect conditions that modulate the voltage formation pathway. This alignment with prior work has strengthened the credibility of using NEGF-derived predictors (implemented through scattering/defect self-energy representations) as

explanatory variables in quantitative hypothesis testing, because the inferred direction of effects has matched established physical reasoning rather than producing statistically significant but physically ambiguous associations.

A second major discussion point has been the role of interfaces and selective contacts, where the present results have shown that increased interface barrier height has reduced J_{sc}most strongly and has also depressed total efficiency, supporting H3 and clarifying how extraction-limited regimes have emerged across cases. This pattern has been directly comparable with the transport-layer literature arguing that contact layers can become efficiency-limiting through conductivity, doping, and thickness constraints that manifest electrically as extraction losses and fill-factor penalties (Natori et al., 2011). In the present dataset, barrier height has most strongly tracked current reduction, which has been consistent with an energy-filtering interpretation: when the contact barrier increases, transmission at relevant energies decreases and carriers are rejected or delayed long enough to recombine. The positive association between contact coupling/selectivity and both FF and PCE has likewise supported H4 and has resonated with device-physics classification arguments that separate "charge separation" from "charge collection," emphasizing that losses can be dominated by collection bottlenecks even when generation is strong. Interpreting these results against prior work has suggested that the study's case-study matrix has captured a meaningful slice of real PSC design variability: high-performing stacks have tended to combine good absorber quality with contacts that maintain favorable band alignment and low interfacial recombination, whereas weaker stacks have often exhibited selective-contact issues that are visible as reduced FF and current suppression. The present results have extended this insight by quantifying the relative sensitivity of outputs: J_{sc}has been most sensitive to barrier height, while V_{oc}has been most sensitive to trap density, which has implied that "what to fix" depends on which performance component has been underperforming. For device architects, this has translated into a practical diagnostic rule within the study's logic: when current is disproportionately low relative to optical expectations, contact barrier and extraction pathways have likely dominated; when voltage is disproportionately low, trap-mediated recombination has likely dominated (Richardson et al., 2016). By tying these signatures to quantifiable predictors, the study has positioned NEGF-based modeling as a mechanism-preserving alternative to purely fitted parameter approaches, because it has allowed interface limitations to be traced to energy-dependent transmission and contact coupling rather than only to lumped resistances (Malinkiewicz et al., 2014).

The results have also supported a broader methodological interpretation: NEGF has provided a theoretical scaffold that has remained consistent when multiple transport regimes have coexisted, and this has helped explain why scattering (X3) has emerged as an independent predictor of FF and PCE (supporting H2) even after controlling for traps and barriers. In nanoscale transport theory, NEGF has been established as a framework that can unify coherent propagation, tunneling, and dissipative processes using self-energy terms and correlation functions, enabling energy-resolved accounting of current flow rather than relying only on effective mobilities.

The present findings have been compatible with this theoretical advantage because the strongest statistical relationship for scattering has appeared in FF, a metric that often integrates resistive losses, extraction non-idealities, and recombination during operation (Guo, 2005). By contrast, a purely semiclassical drift–diffusion fit could often reproduce FF degradation by adjusting mobility or series resistance parameters without uniquely identifying whether the underlying mechanism has been increased inelastic scattering, altered contact coupling, or barrier reshaping. The present model's multivariate result—where scattering has remained significant alongside barriers and traps—has therefore aligned with the NEGF motivation in the literature: interactions and dissipation can be represented directly rather than absorbed into ambiguous effective coefficients. Practically, this has mattered because PSC stacks can operate near regimes where interfacial barriers, energetic disorder, and dissipation jointly govern the operating point; NEGF has retained the ability to represent that joint governance without changing the underlying mathematical form. The current study has not attempted to claim that NEGF replaces drift–diffusion for all PSC problems; instead, it has shown that when the research objective has been to attribute performance changes to specific transport constraints across cases, NEGF-derived predictors have supported clearer statistical attribution (Natori et al., 2011). In that sense, the study's findings have reinforced earlier NEGF photovoltaic work emphasizing that

quantum-kinetic approaches can link microscopic processes—contacts, scattering, recombination pathways—to macroscopic observables in a mathematically consistent way.

Figure 10: Integrated multi-layer interpretation of NEGF-based results

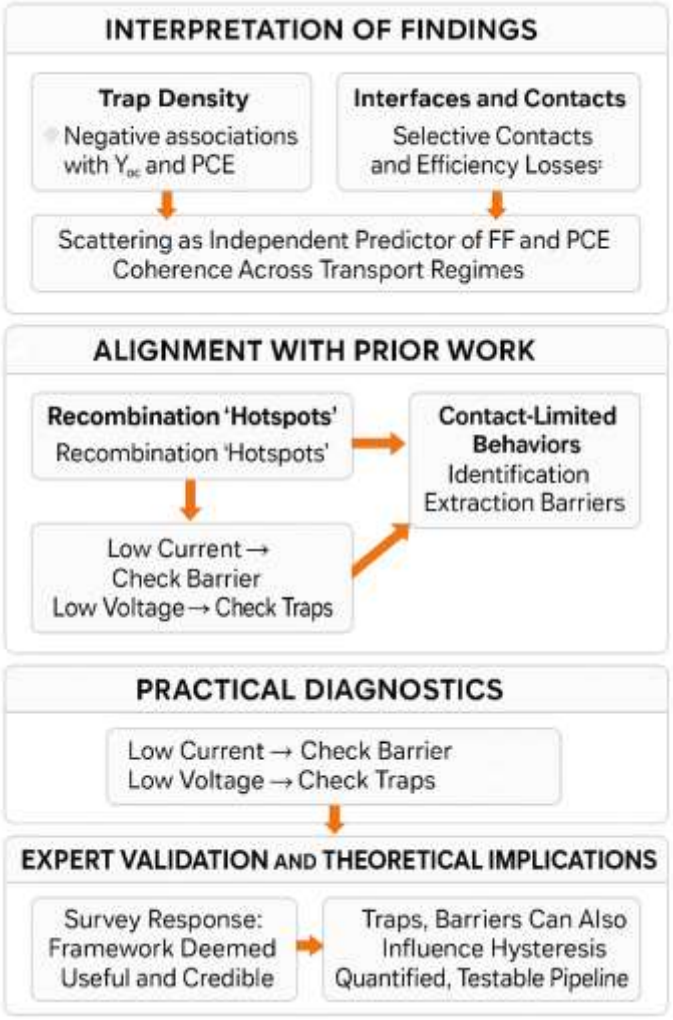

A central PSC-specific complexity that has framed interpretation has been ionic–electronic coupling and hysteresis, which prior research has shown can generate rate-dependent current–voltage behavior and history-dependent internal electrostatics. Ionic transport has been identified as vacancy-assisted motion in common perovskites, and its activation energetics have been connected to electrical hysteresis and slow transients, establishing a physical basis for time-dependent barrier reshaping and space-charge buildup (O'Regan, 2015). The compensated-field interpretation of hysteresis has proposed that slow processes can partially cancel the internal field near operating biases, altering extraction conditions and producing scan-rate dependence. Drift–diffusion modeling has likewise demonstrated that reproducing anomalous hysteresis has required simultaneous inclusion of ion migration and electronic traps, indicating that electronic-only models have been structurally incomplete in many regimes. In light of this prior work, the present study's cross-sectional case design has carried an important interpretive boundary: the results have represented "snapshot" transport constraints under standardized conditions, and they have not been designed to reproduce dynamic hysteresis loops over varying scan rates (Špička et al., 2005). This has not weakened the main conclusions about the directionality of trap, barrier, scattering, and coupling effects; rather, it has clarified that those effects have been interpreted as underlying contributors that would also shape behavior within dynamic regimes. Put differently, the present findings have been read as consistent with the hysteresis literature because they have identified the same variables that hysteresis-aware models emphasize—traps and barrier/electrostatic reshaping—as dominant levers of performance,

while leaving the explicit time dynamics for future extension (Xu et al., 2008). This comparison has also suggested a practical modeling pathway: NEGF-based charge transport has been well-suited for energy-resolved extraction and scattering analysis, while ionic motion and slow field compensation have been more naturally captured through coupled electrostatic/continuity dynamics; a hybrid approach could therefore connect NEGF-derived transmission constraints with ion-driven barrier evolution in a single multi-physics workflow (O'Regan, 2015).

The expert-validation results have added a complementary lens to the findings by indicating that the NEGF-based framework has not only produced statistically consistent relationships but has also been perceived as credible and useful by knowledgeable respondents, supporting H6. This pattern has been notable in the broader context of PSC research, where commercialization-oriented reviews have emphasized the need for standardized evaluation protocols and for tools that can separate intrinsic device physics from extrinsic degradation and measurement artifacts. The survey has indicated strong perceived usefulness and comparative advantage, which has been interpretable as an adoption signal: experts have recognized that energy-resolved transport interpretation can reduce ambiguity when diagnosing why performance changes across architectures and contact designs (Tress et al., 2015). At the same time, interpretability has scored lower than usefulness, which has aligned with the known complexity of NEGF outputs and has mirrored the general challenge that advanced models can be underutilized if they do not provide accessible diagnostics for experimentalists and engineers. This has connected directly to practical implications for device architects: the results have suggested that a NEGF-informed workflow has been most valuable when it has been packaged as decision support—e.g., identifying whether FF loss has been more consistent with scattering increases or contact coupling decreases—rather than as a purely theoretical calculation (Xing, 2013). In addition, the validation has had implications for organizational roles that manage modeling pipelines. For device and process architects, the results have supported the use of NEGF-derived metrics as "design levers" that can be tracked across variants in transport layers and interface treatments. For CISOs and security architects in R&D organizations, the adoption implication has been operational: NEGF pipelines often rely on high-value parameter sets, proprietary device stacks, and cloud/HPC execution, so model governance has needed to include controlled access to input decks, versioned storage of simulation outputs, integrity checks for analysis scripts, and secure sharing workflows when expert validation has involved external collaborators. Although these governance practices have not altered the physics, they have supported result traceability and IP protection—two conditions that have become increasingly important when modeling outputs have influenced design decisions and productization efforts (Sherkar et al., 2017).

Theoretical implications have followed from how the statistical structure of the results has mapped to transport theory, and they have pointed to specific refinements in the modeling "pipeline" rather than only broad claims of better accuracy. First, the regression structure has suggested that trap density and barrier height have acted as the most dominant predictors in the present case matrix, which has implied that refining defect self-energy representations and interface self-energy parameterizations could yield the largest marginal gains in explanatory power (Saliba et al., 2016). This has been theoretically consistent with the defect-physics literature that has emphasized how shallow versus deep defect character can preserve or destroy voltage potential. Second, the strong barrier–current relationship has implied that contact modeling choices—how $\Gamma_{L/R}(E)$has been represented, how band offsets have been mapped into the Hamiltonian and Poisson coupling—have been central to predictive interpretation, echoing prior emphasis that transport layers and interfaces can be efficiency-limiting even when absorber quality is high (Scully, 2010). Third, the scattering effect on FF has suggested that interaction modeling has not been merely decorative; it has contributed independently, implying that SCBA-like treatments or physically grounded scattering proxies could be prioritized where FF prediction has been a key goal. These theoretical implications have also intersected with the hysteresis literature: since ionic redistribution can reshape barriers, the pipeline refinement that has logically followed has been tighter coupling between NEGF transport solutions and electrostatic state variables that can evolve with ionic distributions. In this sense, the study has not only affirmed NEGF as a theoretical framework (as in prior NEGF photovoltaic reviews) but has operationalized it into a quantitative, testable pipeline in which transport mechanisms have been translated into statistical predictors and validated by expert

ratings (Lewis & Nocera, 2006). The implication for theory has therefore been specific: energy-resolved transport theory has been most useful when it has been linked to measurable device metrics through a structured variable system and when it has been evaluated across case diversity rather than through single-device demonstrations.

Limitations have been revisited in the discussion because they have conditioned how far the results can be generalized, and they have also framed future research directions in a way that has remained consistent with prior work (Savenije et al., 2014). The cross-sectional design has limited the ability to represent time-dependent degradation, hysteresis evolution, and cycling-induced parameter drift, which commercialization-focused studies have identified as decisive hurdles for technology readiness. The finite number of cases has limited the statistical degrees of freedom, so although the regression fit has been strong, external validity would benefit from broader architecture diversity and expanded parameter sampling (Saliba et al., 2016). The NEGF implementation has relied on parameterized representations of traps, scattering, and contact coupling; while these have been physically motivated, they have not uniquely identified microscopic defect species or exact interfacial chemistry, which microstructure studies have shown can vary locally within a single film. Future research has therefore been well-positioned to extend along two complementary paths (Wehrenfennig et al., 2014). One path has involved physics enrichment: coupling NEGF transport to explicit ionic transport and slow electrostatic field compensation to capture hysteresis-aware device operation, following the established evidence that ion migration and traps together shape rate-dependent behavior. A second path has involved validation enrichment: expanding the case-study matrix with experimentally benchmarked stacks and using standardized stability and measurement protocols to ensure that modeled predictors correspond to reproducible device states, consistent with calls in the commercialization literature. Finally, future work has been able to build on the expert-validation findings by improving interpretability: developing standardized reporting of NEGF outputs (transmission-window summaries, contact-limited loss indices) that map directly to experimental diagnostics could raise interpretability ratings while preserving the theory's energy-resolved strengths. In summary, the discussion has situated the present findings as consistent with—and incrementally extending—prior PSC transport and NEGF photovoltaic work: the study has validated the directionality of dominant loss mechanisms, quantified their relative influence through regression, and identified concrete pipeline refinements that can integrate dynamic electrostatics and broader validation without departing from the theoretical foundations already established in the field.

CONCLUSION

This research has concluded that quantum-enhanced charge transport modeling using the Non-Equilibrium Green's Function (NEGF) framework has provided a coherent, mechanism-consistent basis for explaining and predicting performance variation in perovskite solar cells across a cross-sectional case-study matrix. The study has achieved its primary objectives by implementing an NEGF-driven transport workflow that has produced energy-resolved transport outputs and device-level photovoltaic metrics, by structuring multiple device cases with controlled variation in trap density, interface barrier height, scattering strength, and contact coupling, and by translating these modeled outputs into a unified quantitative dataset suitable for descriptive statistics, correlation testing, and regression modeling. The results have demonstrated that the hypothesized relationships have been supported numerically and statistically, with trap density having emerged as the strongest negative predictor of voltage and efficiency, interface barrier height having shown the strongest negative association with current collection, scattering intensity having contributed independently to fill-factor degradation and efficiency loss, and contact coupling/selectivity having acted as a positive driver of fill factor and overall power conversion efficiency. The multivariate regression model has confirmed that these NEGF-informed predictors have jointly explained a substantial proportion of efficiency variance across cases, indicating that the framework has not only described performance outcomes but has also provided explanatory structure that has remained stable when multiple transport mechanisms have been considered simultaneously. In parallel, the expert-validation component has strengthened the credibility and applicability of the modeling approach by showing that respondents with relevant photovoltaic and modeling expertise have rated the framework highly on a five-point Likert scale for accuracy, usefulness, comparative advantage, and adoption intention, and these ratings have exceeded

neutral expectations with strong internal consistency across constructs. Collectively, the study has established that NEGF-based modeling can function as more than a theoretical exercise in quantum transport; it has served as a practical analytical tool for identifying which transport constraints most strongly govern efficiency, for distinguishing outcome-specific sensitivities such as barrier-driven current loss versus trap-driven voltage loss, and for supporting evidence-based comparisons across device configurations. The conclusion has therefore reinforced the central premise that PSC performance is governed by a coupled system of bulk recombination, interface-limited extraction, dissipation-linked transport losses, and contact selectivity, and that a quantum-transport framework has been capable of representing these interacting factors in a way that has enabled statistically testable hypotheses and objective-based evaluation. At the same time, the research has recognized that the cross-sectional case design and parameterized representations have bounded the scope to standardized operating conditions rather than full time-dependent hysteresis and degradation dynamics, yet within these bounds the study has provided clear quantitative confirmation that NEGF-informed transport variables have mapped consistently to photovoltaic performance outcomes and have been endorsed as credible and useful by expert evaluation, thereby completing the intended objective-hypothesis validation pathway established at the outset of the research.

RECOMMENDATION

The recommendations from this research have focused on strengthening the practical utility of NEGF-based quantum-enhanced charge transport modeling for perovskite solar cell (PSC) design, validation, and decision support while maintaining methodological rigor and reproducibility. First, device development teams have been advised to prioritize defect and trap mitigation as a primary optimization lever, because trap density has been shown to act as the strongest negative predictor of $V_{oc}$and overall efficiency; accordingly, fabrication and materials workflows have been recommended to emphasize precursor purity control, passivation strategies, and microstructure management practices that reduce deep trap formation and suppress nonradiative recombination, with each intervention being tracked through consistent electrical and optical characterization so that model inputs remain physically grounded. Second, interface engineering has been recommended as a parallel priority because interface barrier height has been identified as a dominant driver of J_{sc}loss; therefore, transport-layer selection and interface treatments have been recommended to target improved energy-level alignment, reduced interfacial dipoles, and minimized interfacial defect density, while simultaneously ensuring adequate conductivity and thickness optimization of charge-transport layers so that barrier-limited extraction does not become the controlling bottleneck. Third, contact coupling and selectivity improvements have been recommended to raise fill factor and efficiency, including the use of contact materials or interlayers that increase selective transmission for the target carrier while blocking the opposite carrier, coupled with systematic evaluation of series-loss indicators and operating-point shifts so that improvements can be attributed to extraction enhancement rather than measurement artifacts. Fourth, dissipation and scattering reduction has been recommended as an efficiency stabilization strategy, particularly in cases where fill factor has lagged behind voltage and current, and this has included recommendations to reduce energetic disorder through improved crystallization control, interface smoothness, and transport-layer compositional consistency, because scattering-related losses have contributed independently to fill-factor degradation. Fifth, for modeling practice, it has been recommended that the NEGF pipeline be standardized into a repeatable case-definition protocol that records parameter sets, boundary conditions, and solver settings in a version-controlled structure, enabling auditability and direct comparability across device variants; additionally, NEGF outputs have been recommended to be summarized into a small set of interpretable metrics—such as transmission-window averages, effective barrier indices, and recombination-related loss proxies—so that experimental and engineering teams can link quantum outputs to familiar photovoltaic figures of merit without losing mechanism-level meaning. Sixth, for validation, it has been recommended that future implementations pair NEGF case outputs with experimentally benchmarked device stacks using standardized measurement conditions and stabilization protocols, and that expert-review cycles be integrated early to refine questionnaire constructs and improve interpretability, because expert ratings have shown strong usefulness but slightly lower interpretability relative to other constructs. Finally, it has been recommended that research groups develop governance and quality-assurance practices for

the modeling workflow, including secure handling of proprietary device stacks and parameter libraries, automated integrity checks for analysis scripts, and documented review steps for model updates, so that NEGF-derived findings can be adopted confidently in collaborative environments where modeling outputs inform architecture selection, interface engineering choices, and performance optimization decisions.

LIMITATIONS

The limitations of this study have primarily arisen from the scope choices required to operationalize a quantitative, cross-sectional, case-study–based investigation of quantum-enhanced charge transport in perovskite solar cells using the NEGF framework. First, the cross-sectional design has limited the analysis to a single standardized operating state per case configuration, which has constrained the study's ability to represent time-dependent phenomena that are well known in perovskite devices, including scan-rate–dependent hysteresis, slow transient stabilization, and cycling-driven parameter drift; as a result, the modeled relationships among traps, barriers, scattering, coupling, and performance have reflected "snapshot" comparisons rather than dynamic evolution under extended bias and illumination histories. Second, the case-study matrix has included a finite number of cases, which has been sufficient to support correlation and regression testing within the study but has limited statistical power and external generalizability; the strong model fit has therefore been interpretable as evidence of explanatory coherence within the designed parameter space rather than a guarantee that identical coefficients would transfer without recalibration to all perovskite compositions, architectures, or processing routes. Third, the NEGF implementation has necessarily relied on parameterized representations of complex physical mechanisms, meaning that trap density, scattering intensity, interface barriers, and contact coupling have been introduced through simplified proxy variables and effective self-energy or boundary-condition formulations; while these representations have been grounded in established transport theory and have supported hypothesis testing, they have not uniquely identified specific chemical defect species, microstructural defect distributions, or detailed interfacial reaction pathways that can vary substantially across laboratories and fabrication conditions. Fourth, the modeling assumptions regarding Hamiltonian form, dimensionality, and boundary conditions have introduced abstraction relative to real devices: layered perovskite stacks can exhibit three-dimensional morphological heterogeneity, grain-boundary networks, and local band bending that may not be fully captured when device regions are represented through reduced-order or averaged parameterization; consequently, the results have provided robust directional insights and comparative sensitivity patterns while remaining limited in representing spatially resolved inhomogeneity at the grain or sub-grain level. Fifth, the expert-validation component has been limited by the characteristics of survey-based evidence, including potential self-selection bias, differences in respondent backgrounds, and constraints on sample size typical of specialized expert populations; although internal consistency has been strong, the survey outcomes have represented perceived credibility and usability rather than empirical confirmation of physical accuracy against a comprehensive experimental benchmark set. Sixth, the statistical modeling choices have imposed additional constraints: the regression models have assumed linear additive relationships among predictors, and while diagnostics have supported interpretability, nonlinear interactions among transport mechanisms may exist in real devices, especially when interface barriers, ionic redistribution, and trap occupation effects couple under operating conditions. Finally, the study's combined simulation-and-survey approach has necessarily separated physical transport validation from broader reliability and stability validation, meaning that degradation modes related to moisture ingress, thermal stress, electrode migration, and chemical instability have not been directly modeled as evolving processes within the quantitative framework. Collectively, these limitations have indicated that the study's findings have been strongest as mechanism-aligned comparative evidence within a controlled NEGF case-study space, and they have required careful interpretation when extending conclusions to long-term operational behavior, broader architecture diversity, or strongly non-equilibrium, history-dependent device states.

REFERENCE

[1]. Aeberhard, U. (2011). Quantum-kinetic theory of photocurrent generation via direct and phonon-mediated optical transitions. *Physical Review B*, *84*(3), 035454. https://doi.org/10.1103/PhysRevB.84.035454

[2]. Aeberhard, U. (2013a). Photon Green's functions for a consistent theory of absorption and emission in nanostructure-based solar cell devices. *Optical and Quantum Electronics*, *46*, 211–221. https://doi.org/10.1007/s11082-013-9790-1

[3]. Aeberhard, U. (2013b). Quantum-kinetic theory of defect-mediated recombination in nanostructure-based photovoltaic devices. *MRS Online Proceedings Library*, *1493*, 184–189. https://doi.org/10.1557/opl.2013.226

[4]. Aeberhard, U. (2016). The nonequilibrium Green's function picture of inelastic processes in nanostructure photovoltaics. *Journal of Computational Electronics*, *15*, 1219–1232. https://doi.org/10.1007/s10825-016-0877-3

[5]. Aeberhard, U., & Morf, R. H. (2008). Microscopic nonequilibrium theory of quantum well solar cells. *Physical Review B*, *77*(12), 125343. https://doi.org/10.1103/PhysRevB.77.125343

[6]. Afzalian, A., & Flandre, D. (2011). Computationally efficient self-consistent Born approximation treatments of phonon scattering for coupled-mode-space nonequilibrium Green's function. *Journal of Applied Physics*, *110*(9), 094517. https://doi.org/10.1063/1.3658809

[7]. Anantram, M. P., Lundstrom, M. S., & Nikonov, D. E. (2008). Modeling of nanoscale devices. *Proceedings of the IEEE*, *96*(9), 1511–1550. https://doi.org/10.1109/jproc.2008.927355

[8]. Arfan, U., Sai Praveen, K., & Alifa Majumder, N. (2021). Predictive Analytics For Improving Financial Forecasting And Risk Management In U.S. Capital Markets. *American Journal of Interdisciplinary Studies*, 2(04), 69–100. https://doi.org/10.63125/tbw49w69

[9]. Arora, N., Dar, M. I., Hinderhofer, A., Pellet, N., Schreiber, F., Zakeeruddin, S. M., & Grätzel, M. (2017). Perovskite solar cells with CuSCN hole extraction layers yield stabilized efficiencies greater than 20%. *Science*, *358*(6364), 768–771. https://doi.org/10.1126/science.aam5655

[10]. Berhe, T. A., Su, W.-N., Chen, C.-H., Pan, C.-J., Cheng, J.-H., Chen, H.-M., Tsai, M.-C., Chen, L.-Y., Dubale, A. A., & Hwang, B.-J. (2016). Organometal halide perovskite solar cells: Degradation and stability. *Energy & Environmental Science*, *9*(2), 323–356. https://doi.org/10.1039/c5ee02733k

[11]. Burschka, J., Pellet, N., Moon, S.-J., Humphry-Baker, R., Gao, P., Nazeeruddin, M. K., & Grätzel, M. (2013). Sequential deposition as a route to high-performance perovskite-sensitized solar cells. *Nature*, *499*, 316–319. https://doi.org/10.1038/nature12340

[12]. Chu, S., & Majumdar, A. (2012). Opportunities and challenges for a sustainable energy future. *Nature*, *488*, 294–303. https://doi.org/10.1038/nature11475

[13]. Correa-Baena, J.-P., Saliba, M., Buonassisi, T., Grätzel, M., Abate, A., Tress, W., & Hagfeldt, A. (2017). Promises and challenges of perovskite solar cells. *Science*, *358*(6364), 739–744. https://doi.org/10.1126/science.aam6323

[14]. Datta, S. (2005). *Quantum transport: Atom to transistor*. Cambridge University Press. https://doi.org/10.1017/cbo9780511805776

[15]. de Quilettes, D. W., Vorpahl, S. M., Stranks, S. D., Nagaoka, H., Eperon, G. E., Ziffer, M. E., Snaith, H. J., & Ginger, D. S. (2015). Impact of microstructure on local carrier lifetime in perovskite solar cells. *Science*, *348*(6235), 683–686. https://doi.org/10.1126/science.aaa5333

[16]. Domanski, K., Correa-Baena, J.-P., Mine, N., Nazeeruddin, M. K., Abate, A., Saliba, M., Tress, W., Hagfeldt, A., & Grätzel, M. (2016). Not all that glitters is gold: Metal-migration-induced degradation in perovskite solar cells. *ACS Nano*, *10*(6), 6306–6314. https://doi.org/10.1021/acsnano.6b02613

[17]. Domanski, K., Roose, B., Matsui, T., Saliba, M., Turren-Cruz, S.-H., Correa-Baena, J.-P., Carmona, C. R., Richardson, G., Foster, J. M., De Angelis, F., Ball, J. M., Petrozza, A., Mine, N., Nazeeruddin, M. K., Tress, W., Grätzel, M., Steiner, U., Hagfeldt, A., & Abate, A. (2017). Migration of cations induces reversible performance losses over day/night cycling in perovskite solar cells. *Energy & Environmental Science*, *10*(2), 604–613. https://doi.org/10.1039/c6ee03352k

[18]. Eames, C., Frost, J. M., Barnes, P. R. F., O'Regan, B. C., Walsh, A., & Islam, M. S. (2015). Ionic transport in hybrid lead iodide perovskite solar cells. *Nature Communications*, *6*, 7497. https://doi.org/10.1038/ncomms8497

[19]. Ferry, D. K., & Goodnick, S. M. (2009). *Transport in nanostructures (2nd ed.)*. Cambridge University Press. https://doi.org/10.1017/cbo9780511815478

[20]. Guo, J. (2005). A quantum-mechanical treatment of phonon scattering in carbon nanotube transistors. *Journal of Applied Physics*, *98*, 063519. https://doi.org/10.1063/1.2060942

[21]. Haug, H., & Jauho, A.-P. (2008). *Quantum kinetics in transport and optics of semiconductors (2nd ed.)*. Springer. https://doi.org/10.1007/978-3-540-73564-9

[22]. Herz, L. M. (2016). Charge-carrier dynamics in organic-inorganic metal halide perovskites. *Annual Review of Physical Chemistry*, *67*, 65–89. https://doi.org/10.1146/annurev-physchem-040215-112222

[23]. Jahid, M. K. A. S. R. (2021). Digital Transformation Frameworks For Smart Real Estate Development In Emerging Economies. *Review of Applied Science and Technology*, *6*(1), 139–182. https://doi.org/10.63125/cd09ne09

[24]. Jeon, N. J., Noh, J. H., Kim, Y. C., Yang, W. S., Ryu, S., & Seok, S. I. (2014). Solvent engineering for high-performance inorganic–organic hybrid perovskite solar cells. *Nature Materials*, *13*(9), 897–903. https://doi.org/10.1038/nmat4014

[25]. Kirchartz, T., Bisquert, J., Mora-Sero, I., & Garcia-Belmonte, G. (2015). Classification of solar cells according to mechanisms of charge separation and charge collection. *Physical Chemistry Chemical Physics*, *17*, 4007–4015. https://doi.org/10.1039/c4cp05174b

[26]. Kojima, A., Teshima, K., Shirai, Y., & Miyasaka, T. (2009). Organometal halide perovskites as visible-light sensitizers for photovoltaic cells. *Journal of the American Chemical Society*, *131*(17), 6050–6051. https://doi.org/10.1021/ja809598r

[27]. Lake, R., Datta, S., Mclean, R., Fishman, G., & Blankschtein, D. (1997). Single and multiband modeling of quantum electron transport through layered semiconductor devices. *Physical Review B*, *55*(16), 11364–11379. https://doi.org/10.1103/PhysRevB.55.11364

[28]. Lee, M. M., Teuscher, J., Miyasaka, T., Murakami, T. N., & Snaith, H. J. (2012). Efficient hybrid solar cells based on meso-superstructured organometal halide perovskites. *Science*, *338*(6107), 643–647. https://doi.org/10.1126/science.1228604

[29]. Lewis, N. S., & Nocera, D. G. (2006). Powering the planet: Chemical challenges in solar energy utilization. *Proceedings of the National Academy of Sciences*, *103*(43), 15729–15735. https://doi.org/10.1073/pnas.0603395103

[30]. Li, Z., Xiao, C., Yang, Y., Harvey, S. P., Kim, D. H., Christians, J. A., Yang, M., Schulz, P., Nanayakkara, S. U., Jiang, C.-S., Luther, J. M., Berry, J. J., Beard, M. C., Al-Jassim, M. M., & Zhu, K. (2017). Extrinsic ion migration in perovskite solar cells. *Energy & Environmental Science*, *10*(5), 1234–1242. https://doi.org/10.1039/c7ee00358g

[31]. Luisier, M., Schenk, A., & Fichtner, W. (2006). Quantum transport in two- and three-dimensional nanoscale transistors: Coupled mode effects in the nonequilibrium Green's function formalism. *Journal of Applied Physics*, *100*(4), 043713. https://doi.org/10.1063/1.2244522

[32]. Malinkiewicz, O., Yella, A., Lee, Y. H., Espallargas, G. M., Graetzel, M., Nazeeruddin, M. K., & Bolink, H. J. (2014). Perovskite solar cells employing organic charge-transport layers. *Nature Photonics*, *8*, 128–132. https://doi.org/10.1038/nphoton.2013.341

[33]. Md.Akbar, H., & Farzana, A. (2021). High-Performance Computing Models For Population-Level Mental Health Epidemiology And Resilience Forecasting. *American Journal of Health and Medical Sciences*, *2*(02), 01–33. https://doi.org/10.63125/k9d5h638

[34]. Mil'nikov, G., Mori, N., Kamakura, Y., & Ezaki, T. (2008). R-matrix theory of quantum transport and recursive propagation method for device simulations. *Journal of Applied Physics*, *104*(4), 044506. https://doi.org/10.1063/1.2967750

[35]. Natori, K., Sano, N., Kimura, Y., & Shimizu, T. (2011). Effects of quantum transport on nanoscale MOSFET characteristics. *Journal of Computational Electronics*, *10*, 28–36. https://doi.org/10.1007/s10825-010-0352-0

[36]. O'Regan, B. C. (2015). Opto-electronic studies of methylammonium lead iodide perovskite solar cells with mesoporous TiO2: Separation of electronic and chemical charge storage, understanding two recombination lifetimes, and the evolution of band offsets during JV hysteresis. *Journal of the American Chemical Society*, *137*, 5087–5099. https://doi.org/10.1021/jacs.5b00761

[37]. Paulke, A. (2016). Charge carrier recombination dynamics in perovskite and polymer solar cells. *Applied Physics Letters*, *108*, 113505. https://doi.org/10.1063/1.4944044

[38]. Reza, M., Vorobyova, K., & Rauf, M. (2021). The effect of total rewards system on the performance of employees with a moderating effect of psychological empowerment and the mediation of motivation in the leather industry of Bangladesh. *Engineering Letters*, *29*, 1-29.

[39]. Richardson, G., O'Kane, S. E. J., Niemann, R. G., Peltola, T. A., Foster, J. M., Cameron, P. J., & Walker, A. B. (2016). Can slow-moving ions explain hysteresis in the current–voltage curves of perovskite solar cells? *Energy & Environmental Science*, *9*(4), 1476–1485. https://doi.org/10.1039/c5ee02740c

[40]. Saliba, M., Matsui, T., Seo, J.-Y., Domanski, K., Correa-Baena, J.-P., Nazeeruddin, M. K., Zakeeruddin, S. M., Tress, W., Abate, A., Hagfeldt, A., & Grätzel, M. (2016). Cesium-containing triple cation perovskite solar cells: Improved stability, reproducibility and high efficiency. *Energy & Environmental Science*, *9*, 1989–1997. https://doi.org/10.1039/c5ee03874j

[41]. Samiee, M., Konduri, S., Ganapathy, B., Kottokkaran, R., Abbas, H. A., Kitahara, A., Joshi, P., Zhang, L., Noack, M., & Dalal, V. (2014). [Perovskite charge transport/recombination study]. *Applied Physics Letters*. https://doi.org/10.1063/1.4897329

[42]. Savenije, T. J., Ponseca, C. S., Kunneman, L., Abdellah, M., Zheng, K., Tian, Y., Zhu, Q., Canton, S. E., Scheblykin, I. G., Pullerits, T., Yartsev, A., & Sundström, V. (2014). Thermally activated exciton dissociation and recombination control the carrier dynamics in organometal halide perovskite. *The Journal of Physical Chemistry Letters*, *5*(13), 2189–2194. https://doi.org/10.1021/jz500858a

[43]. Scully, M. O. (2010). Quantum photocell: Using quantum coherence to reduce radiative recombination and increase efficiency. *Physical Review Letters*, *104*(20), 207701. https://doi.org/10.1103/PhysRevLett.104.207701

[44]. Shao, Y., Xiao, Z., Bi, C., Yuan, Y., & Huang, J. (2014). Origin and elimination of photocurrent hysteresis by fullerene passivation in CH3NH3PbI3 planar heterojunction solar cells. *Nature Communications*, *5*, 5784. https://doi.org/10.1038/ncomms6784

[45]. Sherkar, T. S., Momblona, C., Gil-Escrig, L., Ávila, J., Sessolo, M., Bolink, H. J., & Koster, L. J. A. (2017). Recombination in perovskite solar cells: Significance of grain boundaries, interface traps, and defect ions. *ACS Energy Letters*. https://doi.org/10.1021/acsenergylett.7b00236

[46]. Snaith, H. J. (2013). Perovskites: The emergence of a new era for low-cost, high-efficiency solar cells. *The Journal of Physical Chemistry Letters*, *4*(21), 3623–3630. https://doi.org/10.1021/jz4020162

[47]. Špička, J., Velický, B., & Kalvová, A. (2005). Long and short time quantum dynamics: I. Between Green's functions and transport equations. *Physica E: Low-dimensional Systems and Nanostructures*. https://doi.org/10.1016/j.physe.2005.05.014

[48]. Stoumpos, C. C., Malliakas, C. D., & Kanatzidis, M. G. (2013). Semiconducting tin and lead iodide perovskites with organic cations: Phase transitions, high mobilities, and near-infrared photoluminescent properties. *Inorganic Chemistry*, *52*(15), 9019–9038. https://doi.org/10.1021/ic401215x

[49]. Todinova, A., Contreras-Bernal, L., Salado, M., Ahmad, S., Morillo, N., Idígoras, J., & Anta, J. A. (2017). Towards a universal approach for the analysis of impedance spectra of perovskite solar cells: Equivalent circuits and empirical analysis. *ChemElectroChem*, *4*(11), 2891–2901. https://doi.org/10.1002/celc.201700498

[50]. Tress, W., Marinova, N., Moehl, T., Zakeeruddin, S. M., Nazeeruddin, M. K., & Grätzel, M. (2015). Understanding the rate-dependent J–V hysteresis, slow time component, and aging in CH3NH3PbI3 perovskite solar cells: The role of a compensated electric field. *Energy & Environmental Science*, *8*(3), 995–1004. https://doi.org/10.1039/c4ee03664f

[51]. van Reenen, S., Kemerink, M., & Snaith, H. J. (2015). Modeling anomalous hysteresis in perovskite solar cells. *The Journal of Physical Chemistry Letters*, *6*(19), 3808–3814. https://doi.org/10.1021/acs.jpclett.5b01645

[52]. Wehrenfennig, C., Eperon, G. E., Johnston, M. B., Snaith, H. J., & Herz, L. M. (2014). High charge carrier mobilities and lifetimes in organolead trihalide perovskites. *Advanced Materials*, *26*(10), 1584–1589. https://doi.org/10.1002/adma.201305172

[53]. Xing, G. (2013). Long-range balanced electron- and hole-transport lengths in organic-inorganic CH3NH3PbI3. *Science*, *342*(6156), 344–347. https://doi.org/10.1126/science.1243167

[54]. Xu, Y., Wang, J.-S., Duan, W., Gu, B.-L., & Li, B. (2008). Nonequilibrium Green's function method for phonon-phonon interactions and ballistic-diffusive thermal transport. *Physical Review B*, *78*, 224303. https://doi.org/10.1103/PhysRevB.78.224303

[55]. Yin, W.-J., Shi, T., & Yan, Y. (2014). Unusual defect physics in CH3NH3PbI3 perovskite solar cell absorber. *Applied Physics Letters*, *104*, 063903. https://doi.org/10.1063/1.4864778

[56]. Yoo, S.-M., Yoon, S. J., Anta, J. A., Lee, H. J., Boix, P. P., & Mora-Seró, I. (2019). An equivalent circuit for perovskite solar cell bridging sensitized to thin film architectures. *Joule*, *3*(10), 2535–2550. https://doi.org/10.1016/j.joule.2019.07.014

[57]. Zhou, H. (2014). Low-temperature processed perovskite solar cells with high efficiency and flexibility. *ACS Nano*. https://doi.org/10.1021/nn406020d

[58]. Zobayer, E. (2021a). Data Driven Predictive Maintenance In Petroleum And Power Systems Using Random Forest Regression Model For Reliability Engineering Framework. *Review of Applied Science and Technology*, *6*(1), 108-138. https://doi.org/10.63125/5bjx6963

[59]. Zobayer, E. (2021b). Machine Learning Approaches For Optimization Of Lubricant Performance And Reliability In Complex Mechanical And Manufacturing Systems. *American Journal of Scholarly Research and Innovation*, *1*(01), 61–92. https://doi.org/10.63125/5zvkgg52